

# **Correlation of Part Orientation during 3D-Printing and the Mechanical Properties of Stainless-Steel Alloy**



Author

**Mohammad Umar Safir**

Registration Number **362143**

Supervisor

**DR ADNAN MUNIR**

DEPARTMENT OF MECHANICAL ENGINEERING  
SCHOOL OF MECHANICAL & MANUFACTURING ENGINEERING  
NATIONAL UNIVERSITY OF SCIENCES AND TECHNOLOGY  
ISLAMABAD

**January 2024**

Correlation of Part Orientation during 3D-Printing and the Mechanical  
Properties of Stainless-Steel Alloy

Author

Mohammad Umar Safir

Regn Number

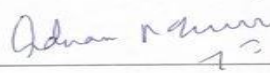
362143

A thesis submitted in partial fulfillment of the requirements for the degree of  
MS Mechanical Engineering

Thesis Supervisor:

Dr. Adnan Munir

Thesis Supervisor's Signature: \_\_\_\_\_



Dr. Adnan Munir  
Assistant Professor  
NUST School of Mechanical &  
Manufacturing Engineering,  
Islamabad, Pakistan

DEPARTMENT of Mechanical Engineering  
SCHOOL OF MECHANICAL & MANUFACTURING ENGINEERING  
NATIONAL UNIVERSITY OF SCIENCES AND TECHNOLOGY,  
ISLAMABAD  
JANUARY 2024

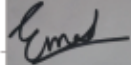
## THESIS ACCEPTANCE CERTIFICATE

Certified that final copy of MS/MPhil thesis written by Regn No. 00000362143 Mohammad Umar Saifir of School of Mechanical & Manufacturing Engineering (SMME) (SMME) has been vetted by undersigned, found complete in all respects as per NUST Statues/Regulations, is free of plagiarism, errors, and mistakes and is accepted as partial fulfillment for award of MS/MPhil degree. It is further certified that necessary amendments as pointed out by GEC members of the scholar have also been incorporated in the said thesis titled. **Correlation of Part Orientation during 3D-Printing and the Mechanical Properties of Stainless Steel Alloy**

Signature: 

Name (Supervisor): Adnan Munir

Date: 19 - Dec - 2023

Signature (HOD): 

Date: 19 - Dec - 2023

Signature (DEAN): 

Date: 19 - Dec - 2023

### Declaration

I certify that this research work titled "*Correlation of Part Orientation during 3D-Printing and the Mechanical Properties of Stainless-Steel Alloy*" is my own work. The work has not been presented elsewhere for assessment. The material that has been used from other sources it has been properly acknowledged / referred.



Signature of Student

Mohammad Umar Safir

2021-NUST-MS-Mech-00000362143

Dr. Ahmad Usman  
Assistant Professor  
Department of Mechanical Engineering  
National University of Science and Technology  
Islamabad, Pakistan

## **Copyright Statement**

- The author retains the copyright for the textual content of this thesis. Reproduction, whether in full or in part, is permissible only in accordance with the author's provided instructions and must be lodged in the Library of NUST School of Mechanical & Manufacturing Engineering (SMME). For specific details, kindly consult the Librarian. Any reproductions must include this page. Additional reproductions, by any means, require the written permission of the author.
- Intellectual property rights related to any content described in this thesis are owned by NUST School of Mechanical & Manufacturing Engineering, unless a prior agreement states otherwise. Third-party use of such intellectual property requires written permission from the SMME, which will specify the terms and conditions of any agreement.
- For further details on the conditions governing disclosures and exploitation, please contact the Library of NUST School of Mechanical & Manufacturing Engineering in Islamabad.

## **Acknowledgements**

I am incredibly grateful to Almighty Allah, the most Generous, Merciful, and Kind One who gave me the fortitude and bravery to finish this research.

I acknowledge and appreciate the guidance and valuable suggestions of Dr. Adnan Munir and Dr. Aqeel Ahsan Khurram under whose supervision, this study has been completed. The author highly acknowledges their co-operation and friendly way of interaction which made this study joyful despite all the difficulties that were experienced. Beside these, I am thankful for the honorable GEC members Dr. Emad ud Din, Dr. Riaz Ahmad Khan, Dr. Muhammad Salman Khan and all the family and friends' prayers and help and last but not the least all the lab engineers and attendants that made this study possible.

*Dedicated to my exceptional parents (Mr. & Mrs. Dr. Muhammad Safir Uddin), adored sibling and loving wife for their unending love and support which lead to the completion of this thesis.*

## **Abstract**

This thesis explores the relationship between the positioning of components during 3D printing and the resulting mechanical and microstructural characteristics of SS-316L alloy, both in its untreated and heat-treated states. Specifically, the study focuses on additive technology implemented at two distinct locations: the stitching line and the center of the print bed using the FS421M additive metal melting system. The current body of literature on the mechanical properties of SS-316L lacks sufficient research on the linked effects of component placement and heat treatment. To address this gap, the authors conducted a comprehensive investigation, presenting original findings. SS-316L is commonly used in applications requiring exceptional resistance to corrosion and high temperatures, and its reduced carbon content enhances resistance to inter-granular corrosion. For evaluating the mechanical properties uniaxial tensile tests and Vickers Hardness tests were conducted at the authors' university. Statistical analysis encompassed factors such as print direction, heat treatment, stress relieving, ultimate tensile strength, yield strength, and specified values. The fracture surfaces were scrutinized using scanning electron microscopy and digital microscopy. The results demonstrate that mechanical properties were affected by the orientation and placement of the samples on the print bed, even when subjected to identical heat treatments. In conclusion, this research highlights the interrelation between part placement in 3D printing and the resulting mechanical and microstructural properties of SS-316L enabling improved practices in additive manufacturing applications.

**Keywords:** Select Laser Melting; Stainless Steel 316L; Part Orientation; Ultimate Tensile Strength; Vickers Hardness; Scanning Electron Microscopy



## Table of Contents

<b>Thesis acceptance Certificate.....</b>	<b>i</b>
<b>Declaration.....</b>	<b>ii</b>
<b>Copyright Statement.....</b>	<b>iii</b>
<b>Acknowledgements .....</b>	<b>iv</b>
<b>Abstract .....</b>	<b>vi</b>
Chapter 1 Introduction.....	1
1.1 Overview:.....	4
1.2 Objectives: .....	5
1.3 Motivation:.....	5
1.4 Future Aspects and Applications: .....	6
Chapter 2 Literature Review.....	8
2.1 3D Printing Technologies: .....	8
2.2 Gaps in Current Knowledge.....	9
2.3 Previous Studies & Practices of Additive Manufacturing and Mechanical Properties..	10
2.4 ASTM Standard.....	16
Chapter 3 Research Methodology .....	17
3.1 Introduction to Research Methodology.....	17
3.2 Significance of Investigating Part Orientation and Mechanical Properties.....	18

3.3 Design of Sample.....	21
3.3.1 Support Structures.....	23
3.3.2 Block Supports.....	25
3.4 Format of Sample.....	26
3.5 3D Printer.....	27
3.6 Material Properties of SS-316L.....	28
3.6.1 Stainless Steel Alloys.....	29
3.6.2 Composition of SS-316L.....	30
3.6.3 Processing Parameters.....	32
3.6.4 Powder Characterization.....	34
3.7. Mechanical Testing.....	35
3.7.1 Why Hardness Test?.....	37
3.7.2 Tensile Test.....	38
3.8 Characterization.....	40
3.8.1 Fractographic Analysis.....	40
3.8.2 Microscopic Analysis.....	41
3.9. Post Processing.....	43

3.9.1. Grinding .....	43
3.9.2. Polishing.....	45
3.9.3. Etching.....	46
3.10 Impact of Heat Treatment.....	49
Chapter 4 Results and Analysis .....	51
4.1 Tensile Strength .....	51
4.2. Vickers Micro Hardness Testing.....	55
4.3 SEM Images of the sample.....	56
4.4 Digital Microscope Images.....	61
4.5 Energy-dispersive X-ray spectroscopy (EDS) Images.....	63
Chapter 5 Conclusion and Recommendations.....	68
5.1 Conclusion: .....	68
5.2 Recommendations:.....	71

## **List of Figures**

Figure 1: Basic workflow of AM

Figure 2: Concept of SLM Process

Figure 3: Additive Manufacturing process.

Figure 4: AM Process

Figure 5: Position of dog-bone samples on the print-bed

Figure 6: 3D Model of Dog-Bone Sample with Block supports.

Figure 7: UTS Testing

Figure 8 & 9: Olympus Corporation DSX1000 UZH Digital Microscope

Figure 10: Scanning Electron Microscope (ZEISS Sigma 500 VP, NCP)

Figure 11: Original Samples after EDM wire cut.

Figure 12: UTS Testing of Samples

Figure 13: Force vs % Elongation

Figure 14 (a – l): Scanning Electron Microscope images.

Figure 15: Defects involved in SLM Printing

Figure 16: (a – h): Digital Microscopic Images.

Figure 17: EDX Graphs (a – d)

## **List of Tables**

Table 1: Literature Review Table

Table 2: Composition of SS-316L

Table 3: Processing Parameters input into the machine.

Table 4: Material Properties of SS-316L

Table 5: Experimental values of Ultimate Tensile Strength, Yield Strength, %  
Elongation at Break (%) & Elongation Rate (%)

Table 6: Experimental Results of all FML composites

Table 6: Vickers Hardness Testing

# Chapter 1

## Introduction

Additive Manufacturing (AM) has emerged as a highly versatile manufacturing technique, offering the capability to produce a diverse array of part geometries. This method employs a meticulous layer-by-layer or particle-by-particle approach to selectively build up single or multi-materials directly from a digital data model, typically in the form of a Computer-Aided Design (CAD) file. A specific and noteworthy application within the realm of AM is Selective Laser Melting (SLM). This particular process is designed for the production of metal components, utilizing metallic powders as the raw material [1-6]. In the SLM process, a high-intensity laser serves as the energy source, selectively melting and fusing the metal powder according to the intricate details specified in the CAD data. This precise layering and fusion process is guided by key parameters such as laser power, scanning speed, hatch spacing, and layer thickness. The careful adjustment of these parameters ensures the seamless fusion of melt vectors and layers, resulting in a meticulously crafted final product. To maintain the integrity of the metal parts being produced, the SLM process often takes place in a controlled environment. The building chamber is commonly filled with either nitrogen or argon gas, creating an inert atmosphere that protects the heated metal parts against oxidation. Two fundamental material properties, namely strength and hardness, play a pivotal role in assessing the quality of SLM-produced parts. These properties serve as essential benchmarks, providing valuable insights into the suitability of these parts for a wide range of applications [7]. It's worth noting that beyond the inherent material properties, there exists a significant opportunity for further optimization. By strategically modifying the shape of the component and adjusting its location and orientation on the print-bed, it becomes possible to enhance the strength-to-weight ratio. This optimization not only contributes to the performance of the part but also facilitates reductions in overall costs, weight, and the number of assembly parts—a noteworthy advantage in the realm of advanced manufacturing and engineering.

In the field of Unmanned Aerial Vehicles (UAVs) and drones, there was a notable surge in technological progress during the late 20th century, mirroring the advancements observed in commercial aviation during the same era. Predictions foresaw a significant rise in UAV utilization over the following two decades, prompting aerospace manufacturers to shift their focus towards innovative solutions. Similar to the evolution of larger wide-body aircraft driven by increased air travel demand, the development of UAVs and drones encountered the challenge of meeting expanding requirements. To cater to the escalating demand for more effective and capable UAVs, manufacturers embarked on exploring larger capacities and enhanced functionalities. This undertaking required a delicate equilibrium between heightened payload capacities, safety considerations, and operational costs. In the competitive environment, the pursuit of superior performance gave rise to groundbreaking technologies designed to propel UAVs and drones into unprecedented realms of efficiency. This innovation enables the production of UAV components that excel in impact resistance, fatigue strength, and overall structural integrity, contributing significantly to the progress of unmanned aerial systems in the contemporary aerospace landscape.

Stainless Steel 316L (SS-316L) powder for additive manufacturing represents a fusion of the strengths found in both metals and composites. Typically, SS-316L powder comprises microscopic particles that are selectively fused layer by layer to form three-dimensional components. This stainless-steel powder offers a combination of corrosion resistance, high strength, and excellent mechanical properties. By harnessing the qualities of SS-316L, additive manufacturing can produce components with superior durability and structural integrity compared to traditional materials. SS-316L powder exhibits remarkable versatility, making it a valuable option across a range of applications due to its exceptional resistance to corrosion. It finds suitability in challenging environments like marine structures, aerospace components, and medical implants. The flexibility of the additive manufacturing process enhances its utility, allowing for the creation of intricate designs and tailored shapes to meet specific engineering needs. At the forefront of advancing additive manufacturing technologies, SS-316L powder boasts improved impact resistance, fatigue strength, and overall durability. This makes it well-suited for applications in aerospace components and medical implants, where it contributes to the production of lightweight yet sturdy structural elements and engine parts. The corrosion-

resistant attributes of SS-316L powder play a significant role in enhancing the longevity and reliability of aircraft structures.

In the medical sector, SS-316L powder is instrumental in producing implants customized to individual patients, leveraging its biocompatibility and resistance to corrosion. Its versatility extends across various industries, establishing it as a compelling choice for additive manufacturing, particularly for components requiring a blend of strength and durability. The diagrammatic representation of SS-316L powder and its additive manufacturing process can be observed in Figure 1, whereas Fig 2 displays the concept of SLM process.

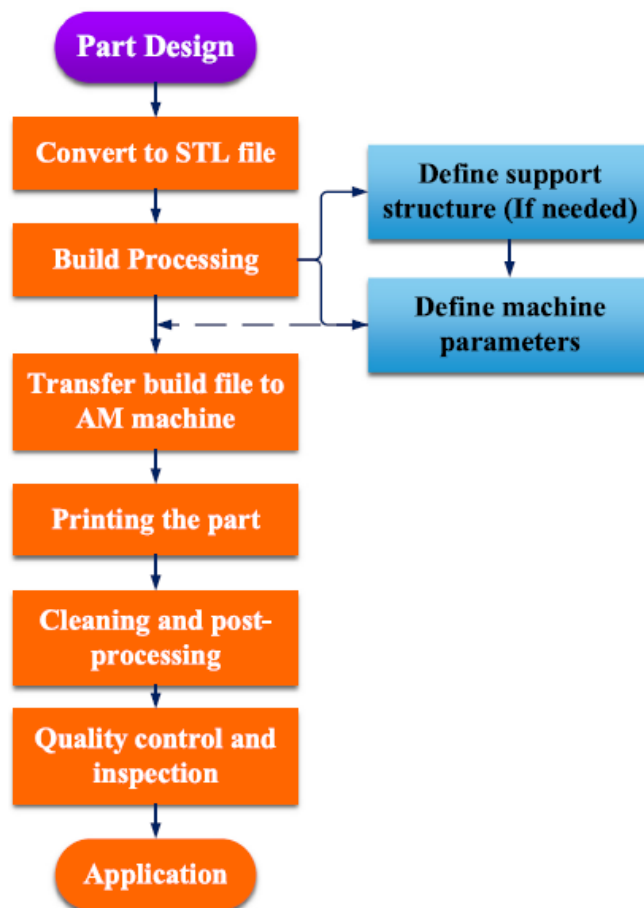


Figure 1: Basic workflow of AM



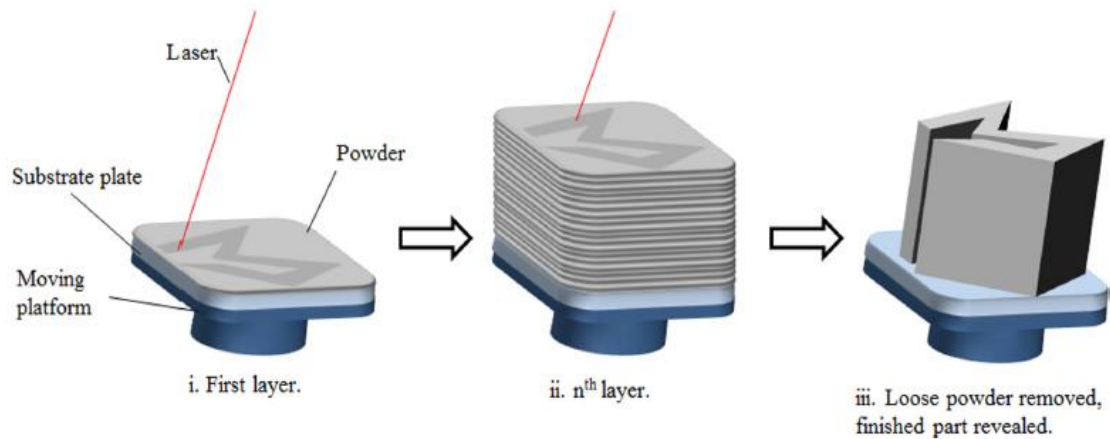


FIG. 2. Concept of SLM process. (i) High-power laser melts selective areas of the powder bed. (ii) Process repeats for successive layers. (iii) Loose powder removed and finished part revealed.

## 1.1 Overview:

The thesis comprises of 5 Chapters. Chapter number 1 gives a concise introduction, covering the objective, motivation & prospects/applications. Chapter number 2 covers The Literature Review educating on the previously performed experimentation in topics related to Metal Additive Manufacturing. Chapter number 3 explains the Methodology and walks through a step-by-step process leading to the completion of this research.

Chapter number 4 displays Results and Discussion based on the results which are achieved by the tests performed on the samples for accurate result-based analysis. Chapter number 4 highlights the key aspects discussed in chapter 4 and gives an informed analysis and review based on the results obtained from the tests. Future Recommendations are also included.

## **1.2 Objectives:**

The Objectives of the thesis are as follows:

1. Design of Tensile Dog-Bone Samples and optimal Support Structure.
2. 3D Printing of Tensile Samples in different orientations and locations on print-bed and its effects.
3. Ultimate Tensile Strength (UTS) Testing and Vickers Hardness Tests for Structural analysis.
4. SEM and Digital Microscopic Imaging for Microstructural and Crack Analysis.

## **1.3 Motivation:**

Powder-based Stainless Steel (SS) - 316L for metal additive manufacturing brings a unique set of qualities to the table. The process of additive manufacturing, especially with metals like SS-316L, allows for intricate and complex designs that might be challenging or impossible with traditional manufacturing methods. Key points that highlight the importance of SS-316L are corrosion resistance, high-temperature strength, and good mechanical properties. The powder-based form retains these properties, making it suitable for applications where durability and resistance to harsh environments are crucial.

These attributes make Metal-AM products extremely desirable for multiple industries majorly to aerospace, automotive, and defense industries, where high strength complex lightweight parts are required. Furthermore, the previous research has developed much deeper insight into the world of metal additive manufacturing and how the processes can be optimized to achieve maximum attainable benefit, results of which showed relatively improved products with higher precision with lower material waste with ability to perform quick iterations and modifications in less time to give a higher strength and durability to endure all the external factors affecting its performance. Focusing on sustainability and advanced manufacturing techniques, research in Metal-AM, has transformed the manufacturing industry by aiding the production of intricate geometries and personalized components with tooling-free production leading to no waste material and high-cost saving. As the adoption of 3D printing with stainless steel alloy continues to grow, it becomes crucial to understand how different printing orientations and

placements on print-bed affect the resulting mechanical properties of the parts. Part orientation refers to the positioning of a component within the printer during fabrication. The orientation of a part can significantly influence its mechanical performance, as the layering and cooling patterns during printing may lead to anisotropic material behavior. Anisotropy refers to the directional dependence of material properties, where mechanical properties may vary along different orientations. Therefore, a thorough investigation of the correlation between part orientation and mechanical properties is essential for improving the process of 3D printing and ensuring the reliability and functionality of the components. Hence, we want to achieve a cost effective, optimized, and efficient method of obtaining high in strength complex structures with high corrosion resistance and durability.

#### **1.4 Future Aspects and Applications:**

Powder-based Stainless Steel for additive manufacturing (Metal-AM) holds significant promise, presenting numerous potential applications across a range of industries. In the aerospace domain, the utilization of Metal-AM for SS-316L offers opportunities to create lightweight components with outstanding strength and damage tolerance. This proves particularly advantageous for crucial aircraft structures such as turbine blades, fuel nozzles, aircraft brackets, engine components, airframe structures, heat exchangers, landing gear components, sensor housings, exhaust components and, fasteners contributing to enhanced performance, fuel efficiency, and overall reliability in aviation.

In the automotive sector, the incorporation of powder-based Metal-AM brings about a transformative shift in vehicle manufacturing. Components made from SS-316L not only contribute to reducing weight and fuel efficiency but also ensure the preservation of structural integrity combined with the material's corrosion resistance with the design flexibility resulting in durable and high-performance automotive parts. The adaptability of SS-316L extends to marine and offshore structures, where its lightweight and ensured resistance to corrosion guarantees overall durability of components, making them well-suited for the challenging conditions of the sea. The ongoing exploration of new and innovative applications through research and development in SS-316L for additive manufacturing establishes it as a versatile and high-performance material for the future.

The continual progress in powder-based Metal-AM opens avenues for diverse industries to harness the benefits of SS-316L, pushing the boundaries of design, functionality, and efficiency.

## Chapter 2

### Literature Review

#### 2.1 3D Printing Technologies

In the realm of additive manufacturing, the envisioned components materialize into tangible objects from a 3D model. This 3D model undergoes conversion into the .STL file format, outlining the external closed surfaces of the original model and serving as the foundation for subsequent slicing calculations. While in STL format, the 3D object remains adaptable, allowing slight modifications such as scaling or optimal orientation.

Furthermore, the component requires support structures, fulfilling roles such as attachment to the build platform, heat conduction, and provision of support in cases of low building angles. These support structures also safeguard the detached part itself. Following the completion of modifications and support generation, both the supports and the part undergo slicing into the format compatible with the Layered Additive Manufacturing (LAM) machine. The layer thickness corresponds to the slice thickness specified in the slice file, typically ranging from 20 to 50  $\mu\text{m}$  for metallic materials in contemporary machines (Gibson, et al., 2010, p. 1-6).

3D printing encompasses a diverse range of technologies. Each technology has its unique features, advantages, and applications. In the context of this thesis on the correlation between part orientation and mechanical properties in stainless-steel alloy 3D printing, it's essential to understand the key techniques that come under the banner of Additive Manufacturing and share the common principle of layer-by-layer material deposition to create three-dimensional objects, which are FDM, SLM, EBM, and Binder Jetting.

Fused Deposition Modeling (FDM) Which is one of the most widely used 3D printing technologies. It involves extruding thermoplastic filaments layer by layer to build the desired object. Selective Laser Melting (SLM) which utilizes a high-power laser to selectively melt and fuse metallic powders, layer by layer, to create metal objects with high precision. It is pertinent to this thesis as it directly involves the additive

manufacturing of metal components, allowing exploration of the influence of part orientation on mechanical properties. Electron Beam Melting (EBM) employs an electron beam to selectively melt and fuse metal powders, like SLM but using an electron beam instead of a laser. Binder Jetting involves selectively depositing a liquid binding agent onto a bed of powder material, layer by layer, to create objects.

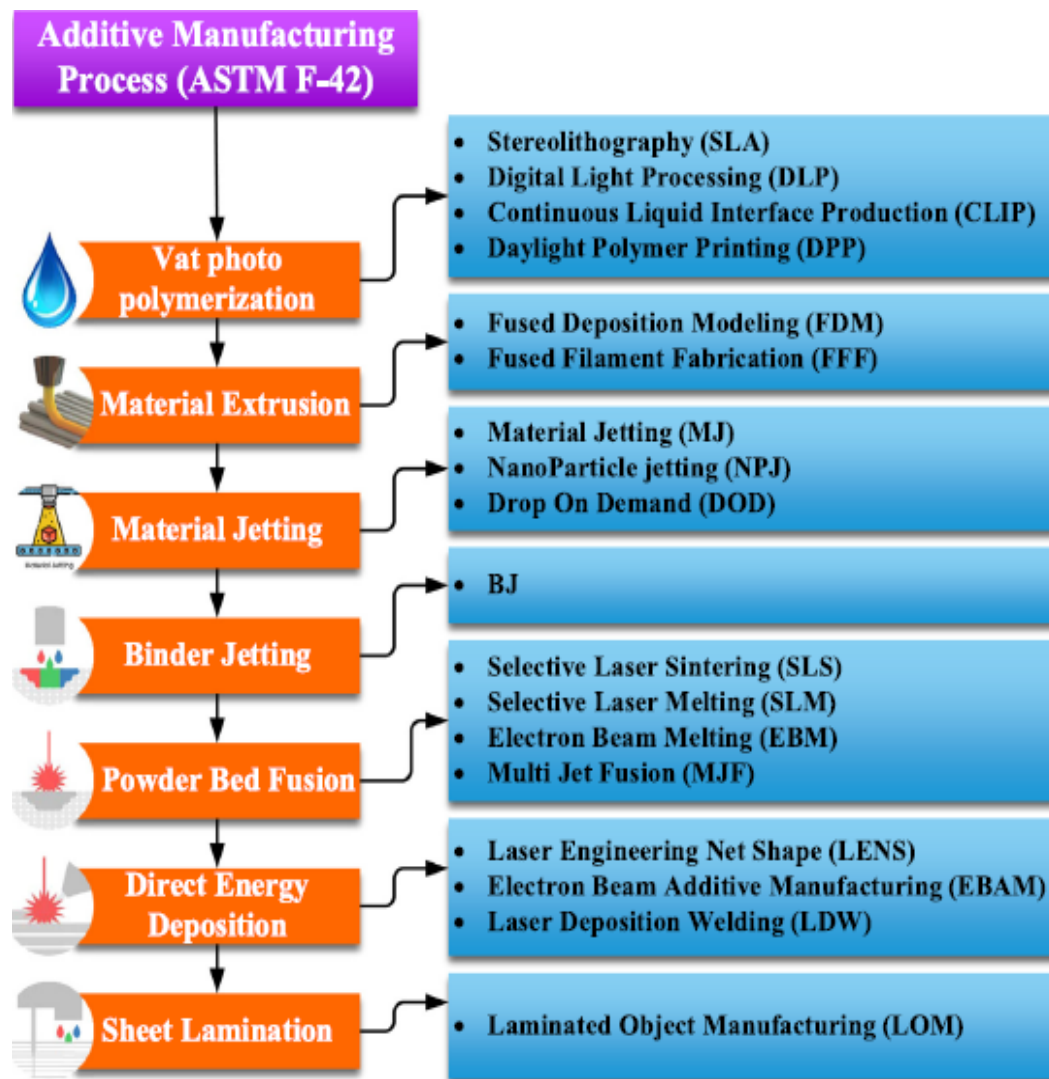


Fig 3. Additive Manufacturing process.

## 2.2 Gaps in Current Knowledge

Examining the existing knowledge gaps underscores the essential need for thorough simulation work and testing across varied conditions, employing diverse methods using

different parameters, orientations, and support structures. The domain of Additive Manufacturing (AM) requires further exploration, specifically in the adoption of alternative materials and support structures. This investigation aims not only to augment strength but also to address the complexities inherent in smaller and intricate components. Moreover, extending the application of this research to advance the capabilities of Unmanned Aerial Vehicles (UAVs) and Aero Components is crucial for enhancing their performance, durability, and resistance to external factors such as elevated altitudes, temperatures, and pressures. Emphasizing different support structures tailored to specific orientations, shapes, and applications is essential. This involves a comprehensive analysis of various parameters and properties associated with both powder and machine process parameters, contributing significantly to the progressive developments in the field.

The inception of this research journey began with an in-depth exploration of existing literature, providing a nuanced understanding of the focal subject, and revealing valuable insights from relevant research papers. Additionally, this literature review not only kindled my interest but also identified a niche for conducting further research. Delving into diverse scholarly works granted me a concise understanding of AM Technologies and the pivotal parameters influencing mechanical and microstructural properties, notably tensile strength, and Hardness. Furthermore, the literature review served as a gateway to diverse AM applications across various industries, such as automotive, aerospace, and construction, unveiling a spectrum of materials tailored for specific purposes.

### **2.3 Previous Studies and Practices of Additive Manufacturing and Mechanical Properties.**

The exploration of existing literature assumes a fundamental role in providing insights into the complex dynamics governing the influence of 3D printing on both mechanical and microstructural properties. A multitude of studies have probed the intricate facets of this phenomenon on the mechanical properties and structural integrity of the part produced, scrutinizing the effects of Printing Machine Parameters, Process Parameters, and Powder Characterization. Notably, the diversity in Printing Methods has been a central focus, with research endeavors directed towards distinguishing the advantages and

limitations inherent in various techniques within the additive manufacturing landscape. Additionally, a significant emphasis has been placed on the comparative analysis of different types of Support Structures and materials for both support structures and build plates. This scrutiny extends beyond the confines of the printing process to encompass a thorough examination of Postprocessing Parameters and Processes, including Heat Treatments and various surface treatments like Polishing, Grinding, and Etching. The cumulative findings derived from studies spanning the reference range [6-16] underscore the pivotal significance of these variables in shaping the overall quality and performance of 3D-printed components. As suggested by the literature, a nuanced comprehension of these parameters and processes is indispensable for attaining optimal outcomes concerning strength, durability, and functionality in the final printed product. The literature review table below highlights all the details involved in the research, i.e., Researchers and Title, experimental setup, conditions, and results.



RESEARCHER & TITLE	EXPERIMENTAL SETUP	CONDITIONS	RESULTS
<p>[7] 2017- Topology-mechanical property relationship of 3D printed strut, skeletal, and sheet based periodic metallic cellular materials.</p>	<p>The considered periodic cellular structures were 3D printed using gas atomized maraging steel fine powder in Powder bed fusion system EOSINT M280 machine supplied by EOS GmbH, Germany. Samples were tested in compression perpendicular to the printing direction.</p>	<p>The particle size of the powder is in the range of 5–50 micro.m.</p> <p>Scanning electron microscope (SEM) was used to assess the quality of printing. Then, samples were tested in uniaxial compression using the Instron and MTS testing machines under displacement-controlled compression.</p>	<p>Most optimum cell topology for best mechanical properties with the least amount of material invested to maximize the stiffness/strength to weight ratio stretching-dominated mode of deformation is observed when the global Orientation of struts were in line with loading direction. All samples showed an increase in the relative density. sheet-Diamond proved to have the best mechanical properties</p>
<p>[8] 2019- Study of 3D printing direction and effects of heat treatment on mechanical properties of MS1 maraging steel</p>	<p>The specimens were built using two different machines – EOS M290 &amp; EOS M280 by DMLS technology. Two testing machines were ZWICK/ROELL Z250 &amp; INSTRON 1362</p>	<p>Process parameters defined by EOS GmbH Standard ‘EOS_DirectTool.’</p> <p>Standard STN EN ISO 6892-1 at ambient temperature (22°C). X, Y, Z direction.</p>	<p>The results showed that it has slightly better properties in the horizontal direction. The outcome of this study pointed rather to the fact that the effect of orientation correlates more with the type of material used rather than with the geometry of the sample. YZ direction is valuable. The best ductility was for samples printed in the X-axis</p>
<p>[9] 2018- Correlation between process parameters, microstructure, and properties of 316 L stainless steel processed by selective laser melting</p>	<p>Test specimens were manufactured using a SLM Realizer II 250 (MPC-HEK) machine equipped with a continuous wavelength (CW Ytterbium fibre laser with spot size of two hundred µm and maximum power of 400 W. The process was conducted under protective atmosphere of high purity argon.</p>	<p>High-density 316 L specimens were successfully fabricated by SLM using laser power values 100W and 200 W, constant scan speed 0.22 m/s and two scanning strategies: alternating stripes without remelting and with re-melting after each layer.</p>	<p>Increase of laser power aligns crystal growth direction with build direction, increases texture degree, increases grain shape aspect ratio, increases fraction of low-angle boundaries, and reduces amount of δ-ferrite. changing of scanning strategy changes one-component cube texture to partially fibre texture, decreases segregation degree and thus suppresses creation of δ-ferrite.</p>

<p>[10] 2021- Prediction of Model Distortion by FEM in 3D Printing via the Selective Laser Melting of Stainless Steel AISI 316L</p>	<p>The orientation position of the 3D printing part was chosen through Autodesk Netfabb software, which contains the Orient Part tool. layer height was set to 0.05 mm. Testing was performed using digital image correlation (DIC).</p>	<p>A Renishaw AM400 3D printer was used to manufacture and test the part. ANSYS Addictive Suite and MSC Simufact Additive for simulation. thermal analysis, structural AM analysis was performed.</p>	<p>Theoretical results were then verified by performing the printing process along with a deformation test. Max Disp=1.5mm. Resulting deformation was slightly higher than the simulated deformation. Verification by a 3D scanner was performed</p>
<p>[11] 2021- Heat treatment effect on the microstructure, mechanical properties, and wear behaviors of stainless steel 316L prepared via selective laser melting</p>	<p>A custom-built powder bed fusion (PBF) was employed to produce SLM SS316L samples. A continuous-wave mode of a 300 W fiber laser (RFL-C300, Raycus Co.) with a central wavelength of 1080 nm and laser beam diameter of 200 μm was used to produce the SLM SS316L. hurrySCAN II 14, SCANLAB) was used for laser beam movement.</p>	<p>(1) a typical furnace-type of heat treatment was conducted at 1100 °C for 0.5 h in a mixture of Ar (100sccm)and H2(10 sccm) atmosphere, followed by furnace cooling. (2) Hot isostatic pressing (HIP, AIP10-30H, AmericanIsostaticPresses) was performed at 1100 °C and 100 MPa for 1.5 h in an Ar atmosphere and gradually cooled down in the furnace.</p>	<p>heat treatments of the SLM samples induced an increase in the density. The EBSD and TEM analyses revealed that the cellular microstructure and dense dislocation structures of the as-SLM disappeared after the short heat treatments owing to recrystallization. The SLM samples showed lower surface-hardness than the conventional CR. Notwithstanding the higher density, the HT-SLM and HIP-SLM showed a relatively lower surface hardness than that of the as-SLM.</p>

<p>[12] 2021- Microstructural and mechanical evaluation of postprocessed SS 316L manufactured by laser-based powder bed fusion</p>	<p>The SS316L specimens of cylindrical bars with a diameter and length of 10 mm and 60 mm were manufactured with an EOS M280. Yb-Fiber laser of 200W maximum power with the laser beam's diameter at 75 mm. The build volume was 250 _ 250 _ 325 mm<sup>3</sup>, and the powder layer's thickness during the building was set at 20 mm. The tensile tests were performed with a Zwick Z5 5 kN Universal Testing Machine</p>	<p>The LPBF parameters were optimized to minimize porosity and defects such as un-melted or partially melted grains. A laser power, scan speed, and hatch spacing of 195 W, 1083 mm/s, and 90 mm, respectively, were applied for specimen fabrication.</p>	<p>The as-built parts contained extremely low porosity levels, as shown in the micro-CT results. The specimens' density levels lie in the range of 99.993e99.997%, with only extremely small pockets of pores present. When the specimens quenched at 1050 _C with the 40 minutes dwelling time, the mechanical properties and fractography characteristics improved due to smaller grain size, better uniformity of fused powder, fewer voids, and defects of the fracture surface.</p>
<p>[13] 2022-Experimental investigation of mechanical properties for wrought and selective laser melting additively manufactured SS316L and MS300</p>	<p>The sample was prepared on the selective laser melting machine from the EOS M280 machine.</p>	<p>The input energy density used for SS316L and MS300 was 58 J/mm<sup>3</sup> and 68 J/mm<sup>3</sup>, respectively. A laser beam was scanned on the predefined path. The samples were printed with strip scanning pattern with 67_ rotation per layer to ensure proper sintering of material. The samples were built in a direction parallel to the vertical building direction (z-axis) with scanning plane</p>	<p>The relative density of a sample has a prominent effect on its mechanical qualities. The SLM additively manufactured (SLMAM) build material with higher density exhibits better tensile properties and impact energy. The SLMAM build samples of SS316L and MS300 show 5–10% higher tensile strength and hardness 15–17 % higher than wrought samples due to the higher cooling rate in SLM process. More Elongation</p>

		<p>parallel to (XY-axis). The samples were removed from the base plate and followed by support material removal with the help of wire cut EDM.</p>	<p>in SLM-AM samples of SS316L and MS300.</p>
<p>[14] 2022- Effects of scanning speeds on the wear behaviour of CoCrW alloy fabricated by selective laser melting</p>	<p>Renishaw AM290 laser melting machine. The microstructure morphology of the sample was observed by FE-SEM-EDS (Zeiss Merlin, Germany)</p>	<p>The anisotropic wear resistance of the CoCrW alloy manufactured by selective laser melting with 3 different scanning speeds was studied. The microstructures of the FD-SD surface and BD-SD surface of SLM CoCrW alloy were analyzed. The influences of the microstructures of SLM CoCrW alloy on the wear behaviors were investigated</p>	<p>The wear rate of the SLM CoCrW alloy FD-SD plane is larger than that of the BD-SD plane. The friction coefficient of the SLM CoCrW alloy BD-SD plane with different laser scanning rates is close, about 0.60. Adhesive wear is the reason for the higher wear rate of the 700 mm/s sample</p>

<p>[15] 2022- Micro selective laser melting of SS316L: Single Tracks, Defects, microstructures, and Thermal/Mechanical properties</p>	<p>self-developed MSLM machine was used for the experiments, Han’s Laser M100. 500 W IPG fiber laser (<math>\lambda = 1.07\mu\text{m}</math>) with a small laser spot size of <math>25\mu\text{m}</math>, a building platform with <math>10\mu\text{m}</math> precision, an automatic powder recoater, building chamber with inert gas protection and a computational process control system.</p>	<p>Aerosolized SS316L powder was used in this experiment. surface profile of the formed single tracks with laser power of (70 ~ 250) W and scanning speed of (200 ~ 3000) mm/s.</p>	<p>Laser power and scanning speed have a significant effect on the continuity of single tracks forming. The optimal process parameters of laser power, scanning speed and hatch spacing are 90 W, 800 mm/s and 0.07 mm, respectively. The mechanical properties of MSLMed SS316L are good with elongation over 40%,</p>
<p>[16] 2023- Investigating the effect of laser shock peening on the wear behaviour of selective laser melted 316L stainless steel</p>	<p>AMPRO SP 500 selective laser melting machine equipped with a Q-switched pulse laser with a spot size of <math>110\mu\text{m}</math> and maximum output power of 500 W.</p>	<p>SLM 316L stainless steel is <a href="#">subjected</a> to LSP, which <a href="#">promotes</a> micro-level <a href="#">grain refinement</a> and compressive residual stresses.</p>	<p>The LSPed specimen exhibits increased micro-hardness and higher wear resistance compared to the polished as-printed specimen. The <a href="#">wear rate</a> of the LSPed specimen is <a href="#">reduced</a> by 26%.</p>

Table 1: Literature Review

## 2.4 ASTM Standards:

ASTM, originally the American Society for Testing and Materials and now recognized as ASTM International, establishes comprehensive guidelines and specifications for testing, evaluating, and guaranteeing the quality and performance of diverse materials and products across industries. In the Manufacturing of SS-316L Samples using SLM method we adhered to two specific ASTM standards. ASTM F-42 was employed for AM Process.

## Chapter 3

### Research Methodology

#### 3.1 Introduction to Research Methodology

This research employs a thorough and multifaceted methodology, divided into distinct stages, to deeply investigate and clarify the intricate dynamics of the subject. The sequential progression of these stages is crucial for a holistic exploration and understanding of the phenomenon under study. The initial phase involves intricately designing the experimental framework, establishing foundational parameters and variables to ensure a systematic and controlled study. Following the design phase, the manufacturing stage unfolds as a pivotal step. Here, theoretical constructs materialize into tangible entities through advanced additive manufacturing techniques, characterized by precision and adherence to predefined design specifications. This stage embodies the translation process from conceptualization to reality.

After manufacturing, a meticulous post-processing regimen commences, addressing intricacies to refine and enhance the fabricated components. This step is instrumental in fine-tuning material properties, ensuring structural integrity, and overall quality. Various post-processing techniques are judiciously applied to optimize desired characteristics and meet stipulated criteria. The subsequent mechanical testing phase is indispensable, subjecting fabricated specimens to a battery of assessments, ranging from tensile strength to hardness. This elucidates nuanced mechanical behavior under varying conditions, employing rigorous testing protocols to derive comprehensive insights into the material's response to applied forces. This facilitates a robust evaluation of its structural efficacy. The final stage involves microscopic analysis, delving into microstructural intricacies using advanced imaging techniques to scrutinize the minutiae of fabricated components. This microscopic scrutiny is paramount for unraveling underlying mechanisms and structural nuances contributing to the material's overall performance. In essence, this research unfolds through thoroughly coordinated stages, each contributing a unique dimension to the principal narrative. The iterative and interconnected nature of these stages fosters a cohesive and exhaustive exploration, transcending individual boundaries

and encapsulating the holistic essence of the research endeavor. The comprehensive research approach is detailed in the following manner.

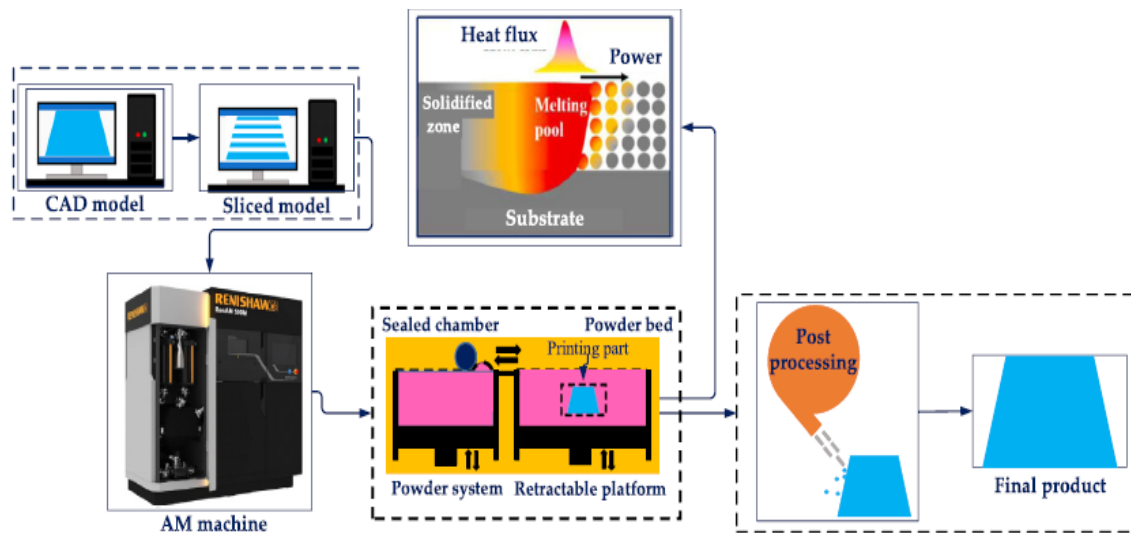


Figure 4: AM Process

### 3.2 Significance of Investigating Part Orientation and Mechanical Properties

Exploring the significance of delving into part orientation and mechanical properties is crucial as it forms the essence of advancing our comprehension of how the alignment of a 3D-printed part during the printing process impacts its subsequent mechanical performance. The orientation of a part within the 3D printing space holds profound implications for its structural integrity, strength, and overall mechanical behavior. This investigation delves into unraveling the intricate connection between the orientation of a printed object and the resulting mechanical properties it exhibits. Systematically examining and understanding the influence of part orientation provides researchers and practitioners with invaluable insights to optimize the printing process tailored to specific applications. This knowledge, in turn, can drive enhancements in the efficiency, reliability, and functionality of 3D-printed components, ushering in progress across diverse industries, from aerospace to healthcare. Moreover, the scrutiny of mechanical properties in conjunction with part orientation aids in establishing guidelines and best practices to achieve desired outcomes in 3D printing. It enables the identification of optimal orientations that minimize vulnerabilities, such as susceptibility to cracks or

distortions, while maximizing the overall performance of printed parts. This knowledge proves instrumental for designers, engineers, and manufacturers aiming to leverage the full potential of 3D printing technology, ensuring the quality and durability of the end products. In summary, exploring the significance of investigating part orientation and mechanical properties is pivotal for unlocking the complete potential of 3D printing technology, furnishing invaluable insights that have the potential to shape the future landscape of manufacturing and design across a spectrum of industries.

The orientation of parts on the print bed in 3D printing is a crucial factor that can significantly influence the mechanical properties and overall quality of the printed objects. In the provided description: The samples were built in a direction parallel to the vertical building direction, often referred to as the Z-axis. This means that the layers of the 3D-printed samples were stacked vertically, one on top of the other. The scanning plane, where the 3D printer's laser or nozzle moves during the printing process, was parallel to the XY-axis. This arrangement ensures that the primary movement of the printing tool is in the horizontal plane. The term "stitching line" refers to the boundary or seam where different layers of metal powder are fused together during the printing process. Placing two samples parallel to the base plate on the stitching line suggests a deliberate investigation into the effects of this specific orientation on the final properties of the printed samples. Two additional samples were placed in the center of the print bed. These were positioned at angles of 0 degrees and 90 degrees. The angle of 0 degrees likely means that the sample is aligned with the default orientation of the print bed, while 90 degrees indicates a perpendicular alignment. This arrangement allows for exploring how different orientations impact the final properties of the printed samples. Consistency and Comparison by specifying the orientation and placement of the samples, the study ensures consistency in the printing process, allowing for a fair comparison of the samples' mechanical properties. The effect of Stitching Line is placing samples on the stitching line provides insights into how this specific feature, where layers are fused together, influences the structural integrity and properties of the printed metal.



Orientation Variation is the deliberate variation in orientation (0 degrees and 90 degrees) helps assess the anisotropic properties of the printed samples, understanding how different orientations may affect strength, hardness, or other mechanical characteristics. In essence, the orientation of parts on the print bed is a carefully considered aspect in this study, allowing for a systematic exploration of how different orientations and positions influence the performance of the 3D-printed metal samples.

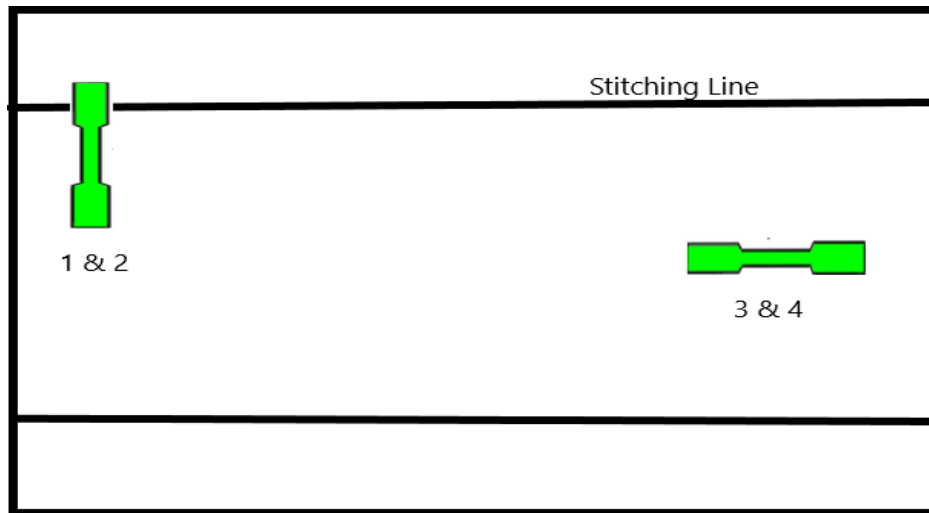


Figure 5: Position of dog-bone samples on the print-bed

The term "Stitching Lines" denotes the specific areas within the metal 3D printing process where distinct layers of metal powder undergo fusion. This fusion occurs because of the selective melting facilitated by a laser, with each layer incrementally contributing to the construction of the ultimate 3D object. In essence, the stitching lines represent the demarcation points where one layer seamlessly integrates with the layer immediately beneath it. The significance of maintaining a high standard of quality for these stitching lines cannot be overstated, as it directly correlates with the structural integrity of the resulting metal part. Meticulous attention to ensuring the precision and cohesion of these boundaries is imperative to guarantee the overall robustness and reliability of the final printed metal component.

### 3.3 Design of Sample

Testing using a dog bone model, also known as a tensile test specimen, holds significance in the field of materials science and engineering for several compelling reasons one of which is that the dog bone shape conforms to standardized testing procedures, ensuring consistency, and facilitating comparisons across different materials and manufacturing processes. This standardization is crucial for reliable and reproducible results. The dog bone model allows for the measurement of stress and strain during a tensile test. This analysis provides fundamental data on the material's behavior under tension, offering insights into its mechanical properties such as tensile strength, yield strength, and modulus of elasticity. By subjecting the dog bone specimen to tension until failure, researchers gain a comprehensive understanding of the material's response to applied forces. This aids in characterizing the material's ductility, brittleness, and overall mechanical behavior, providing valuable information for material selection in engineering applications. The tensile test using a dog bone model is a common quality control practice in manufacturing. It helps ensure that the produced materials meet specified standards and requirements, contributing to the consistency and reliability of manufactured components.

Engineers use data obtained from tensile tests on dog bone specimens to optimize the design of structures and components. Understanding how a material behaves under tension allows for the selection of materials that meet the specific mechanical requirements of a given application. In research and development, the dog bone model serves as a fundamental tool for studying the mechanical properties of new materials. Researchers can assess the performance of novel alloys, composites, or additive manufacturing processes using standardized tensile testing. The simplicity and standardization of the dog bone model make it an excellent educational tool. It is commonly used in materials science and engineering courses to teach students about the principles of tensile testing and the mechanical behavior of materials. The dog bone model serves as a versatile and standardized tool for characterizing the mechanical properties of materials, providing essential data for engineering applications, research, and quality control processes. Its importance lies in its ability to offer a standardized and reproducible means of understanding how materials respond to applied forces, informing decisions in material selection, design, and manufacturing.

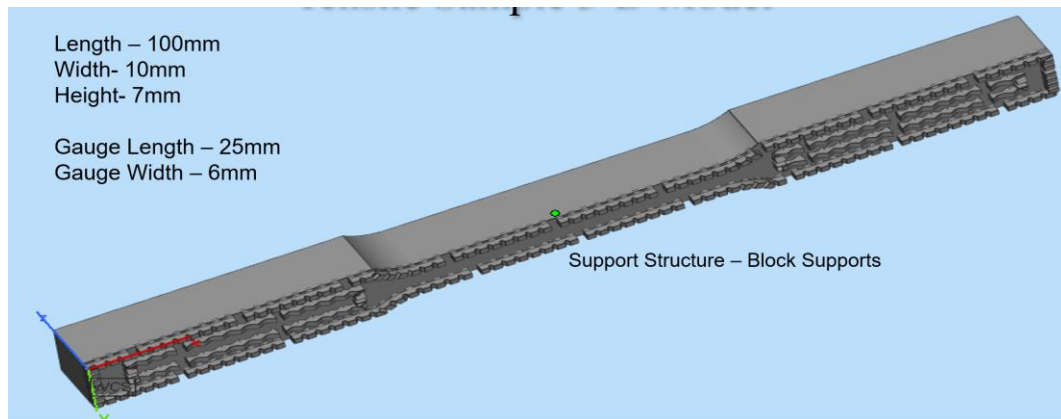


Figure 6: 3D Model of Dog-Bone Sample with Block supports.

Let's break down the dimensions of the dogbone sample and delve into the significance of each dimension. The dimensions of the Dog-bone/Tensile Sample are as follows, Overall Length ( $L_0$ ) is 100mm, the overall length represents the original length of the specimen. During a tensile test, the material undergoes deformation, and understanding the original length is crucial for calculating strain accurately. Width ( $W$ ) is 10mm, the width is the measure across the broader section of the dogbone. It plays a pivotal role in determining the cross-sectional area of the specimen, which is a critical factor in calculating stress (force per unit area). Height ( $H$ ) is 7mm, the height represents the thickness of the specimen. Similar to width, the height influences the cross-sectional area and, subsequently, the stress calculation. It also affects how the material responds to applied forces. Gauge Length ( $L_g$ ) is 25mm, the gauge length is the portion of the specimen where deformation occurs during the tensile test. It's a standardized length used for strain calculations. Knowing the gauge length is essential for accurately determining how much the material has deformed. Gauge Width ( $W_g$ ) of 6mm, the gauge width is the width of the specimen at the gauge section. Like the gauge length, it is a standardized dimension used for calculating strain and, subsequently, stress.

The specified dimensions ensure consistency in testing procedures across different experiments and industries. Standardization allows for meaningful comparisons of material properties. The dimensions, particularly the gauge length and gauge width, are fundamental for calculating stress and strain accurately. This data is vital for understanding how the material behaves under load. The dog bone shape, with its

narrower sections (necks), is designed to induce failure within the gauge length. Analyzing where and how the material fails provides insights into its tensile strength, ductility, and fracture behavior. The data derived from these dimensions is crucial for engineers in various industries. It informs decisions related to material selection, design considerations, and the overall performance of materials under tension. Standardized dimensions are essential in quality control processes, ensuring that materials meet specified standards and can perform as expected in various applications.

In conclusion, the dimensions of the dogbone sample, including overall length, width, height, gauge length, and gauge width, are carefully chosen to facilitate standardized and meaningful tensile testing. This information is invaluable for understanding the mechanical properties of materials, aiding in material selection, and informing engineering decisions.

### **3.3.1 Support Structures**

In the context of SLM in metal 3D printing, support structures have high importance in maintaining the stability and integrity of printed components. These structures serve as anchors to avoid the deformation or collapse due to gravity during production, tethering unconnected parts, and dissipating heat to prevent thermal warping. The success of part production depends heavily on effective support structures that support overhanging features and prevent warpage, influencing the printability and resulting physical and mechanical properties.

Support structures have an integral impact on the successful production of 3D printed metal components, playing a key role in supporting overhangs and mitigating warping. These structures are additional components designed to support specific tasks, including preventing tilting of overhanging features, countering mechanical loads caused by residual stresses, and dissipating process heat. This study delves into the challenges posed by common support structures and emphasizes the need for optimized designs to enhance efficiency and minimize post-processing efforts.

To ensure a successful build, the build plate needs an efficient heat transfer for strong adherence of the part and build plate, minimal material utilization and print duration, trying to avoid the entrapment of the powder, and effortless removal are critical considerations. The choice of support structures significantly impacts the heat transfer during printing, necessitating a balance between material usage and thermal management. The post-processing of parts is also a key aspect, with an emphasis on cost-effective and time-efficient removal. Current challenges in support structures revolve around material wastage, poor manufacturability, and issues with defined geometry, leading to heavy metal dross. Reviewing past approaches highlights the limitations of solid-based and surface-based support structures, necessitating a need for innovative designs that leverage the advantages of both types.

The study employs a comprehensive methodology involving load analysis, topology optimization, and comparisons between 3D printing technologies. The goal is to determine optimal support structures that consider area in contact, volume of the support material, build time, and per unit cost. The comparison involves SLA, FDM, and metal processes, each evaluated based on their specific criteria for successful 3D printing. In-depth investigations into approaches like inclined deposition, removable water/ice support, and multi-axis manufacturing reveal both successes and challenges. The need for innovative designs that combine the strengths of different approaches is evident, aiming to avert printing failures and conserve material, time, and effort both in the printing phase and subsequent post-processing, strategic adjustments in the component's shape, location, and orientation on the print bed prove crucial. This optimization not only enhances the overall strength-to-weight ratio but also yields significant benefits in terms of cost efficiency and streamlined manufacturing processes.

The study concludes with recommendations for future research, emphasizing the need to address the tasks of support structures: supporting overhangs, countering mechanical loads, and dissipating heat. The proposal includes creating a proof of concept utilized for heat dissipation, validating the procedure with complex part geometries, investigating how decreased densities affect structural strength and thermal conductivity. and establishing standardized models for fair comparisons between support methods. The

quest for more economical and efficient support strategies continues, promising advancements in the field of metal 3D printing. [22-27]

### **3.3.2 Block Supports**

Block supports play a pivotal role in the realm of metal 3D printing, as their significance lies in ensuring stability and upholding the structural integrity of the printed object throughout the additive manufacturing process. Let's delve into a comprehensive exploration of the reasons behind the use of block supports and their crucial implications. These supports function as a foundational structure, preventing deformation or collapse during the 3D printing process. Given that metal materials are deposited layer by layer in a molten or semi-molten state, they are susceptible to sagging or distortion. Acting as scaffolding, block supports secure the partially formed object in position until the material solidifies. In intricate 3D designs with overhangs, protrusions, or detailed features, block supports act as transient pillars, facilitating the printer in constructing these challenging geometries, averting potential failures or shape distortions. Metal 3D printing involves substantial heat, with each layer undergoing rapid heating and cooling. Block supports play a role in dissipating excess heat, averting thermal issues such as warping or uneven cooling, which could jeopardize the final structure's quality. As the metal cools and solidifies, it tends to contract, resulting in residual stress within the printed object. Strategically positioned block supports provide controlled areas for thermal contraction, diminishing the likelihood of defects like cracking, warping, or uneven stress distribution. Additionally, block supports contribute to a refined surface finish on the end product by minimizing distortions or deformations during the printing process, ensuring that external features maintain their intended shape and dimensions. Upon completion of metal printing, the removal of support structures becomes imperative. Block supports are meticulously designed for effortless removal without causing harm to the main structure, a crucial feature for achieving the desired final form without post-processing challenges. These supports also play a pivotal role in preserving the accuracy and precision of the 3D print, providing a steadfast foundation that reduces the chances of errors, misalignments, or deviations from the intended design specifications. In essence, block supports emerge as a critical component in metal 3D printing, delivering structural stability, facilitating the fabrication of intricate designs, managing thermal aspects, and contributing significantly

to the overall quality and integrity of the final printed metal object. Their strategic placement and design considerations stand as integral factors determining the success of additive manufacturing processes within the domain of metal fabrication.

### **3.4 Format of Sample**

The design process involved the utilization of SolidWorks software to create the model. Once the design was finalized, the next step was to convert it into an STL (Standard Tessellation Language) file format. This file, containing the detailed digital representation of the model, was subsequently input into the computer of the 3D printer. The transition from the SolidWorks design to the STL file format facilitated seamless communication between the digital model and the 3D printer, allowing for precise and accurate reproduction of the designed object.

Converting a CAD model into STL format before inputting it into a 3D printer is a crucial step in the 3D printing process, and it serves several important purposes. Mesh representation is facilitated because CAD models are typically represented using NURBS (Non-Uniform Rational B-Splines) or other mathematical representations, which are precise and smooth. STL (Stereolithography) format represents 3D geometry as a mesh of triangles. This triangular mesh is more suitable for 3D printing processes. Geometry is simplified since 3D printers work with a layer-by-layer approach, and complex CAD models may contain intricate details that are unnecessary or challenging to reproduce accurately. Converting to STL allows for the simplification of the geometry into a mesh of triangles, making it easier for the 3D printer to interpret and execute. These files provide a clear definition of the surface geometry of the object. The mesh structure outlines the boundaries and surfaces of the model, enabling the 3D printer to precisely recreate each layer during the printing process. The files are typically smaller in size compared to complex CAD files. This optimization is beneficial for storage, transfer, and processing speed during the 3D printing workflow. It is a widely accepted and standardized file format in the 3D printing industry. Most 3D printers recognize and support STL files, making it a universal format for communication between CAD software and 3D printers. Compatibility is ensured because CAD software may have its own proprietary file formats, and not all 3D printers are compatible with these formats.

Converting to STL ensures compatibility between different software and hardware platforms. These files are typically smaller in size compared to complex CAD files. This optimization is beneficial for storage, transfer, and processing speed during the 3D printing workflow. Printing Parameters are defined since STL files include information about the orientation, size, and position of the 3D model. This information is crucial for the 3D printer to know how to construct each layer and build the final object. Error Checking and validation of the model's geometry help identify and rectify any potential issues that may arise during the printing process. In summary, converting a CAD model into STL format is a necessary step to prepare the 3D model for the layer-by-layer printing process. It simplifies geometry, ensures compatibility, and provides a standardized representation that 3D printers can easily interpret and execute.

### **3.5 3D Printer**

The Farsoon FS421M additive metal melting system stands as an advanced solution tailored for continuous production in the realm of metal 3D printing. Boasting a formidable build cylinder measuring 425x425x420mm, the FS421M demonstrates its prowess in manufacturing large metal parts across a diverse range of metal powder materials. The integration of a multi-laser and fully digital optics system not only amplifies production speed but also contributes to the system's capability for enhanced efficiency. Facilitating swift cylinder exchanges between builds is the internal rail system, further emphasizing its commitment to seamless and continuous production. In terms of efficiency and safety, the FS421M introduces a novel closed-looped powder handling system, seamlessly integrating powder supply, transport, feeding, and recycling into a unified inert system. The inclusion of a potent air filtration system not only enables the processing of reactive materials but also extends usage intervals between filter changes, thanks to its high capacity and auto-cleaning feature. Embracing an open system philosophy, the FS421M, like all Farsoon systems, grants users unparalleled freedom by unlocking all machine parameters and adopting an open material policy. This affords unprecedented levels of flexibility and freedom in the realm of additive metal melting production. Additionally, the in-house Farsoon software ensures user-friendly operation, offering both an advanced user interface and a touch screen-based production interface for everyday use. In summary, the FS421M emerges as a robust and versatile solution,



exemplifying a harmonious blend of production efficiency, safety features, and user-friendly design in the domain of metal 3D printing.

This system is adept at producing large metal parts across a diverse range of metal powder materials. With a net weight ranging from approximately 3450kg (Single-laser) to 3500kg (Dual-laser), the FS421M ensures stability and reliability in its operations. It operates with a layer thickness ranging from 0.02 to 0.1 mm, achieving precision in the printing process. The scanning speed, reaching a maximum of 15.2 m/s, enhances production efficiency. The system employs either a dual fiber laser (2×500W) or a single fiber laser (1×500W), with a laser spot size of approximately 70µm contour and 70-200µm fill, ensuring accuracy in the printing details. With base-plate heating at 200°C and inert gas protection using Argon/Nitrogen, the FS421M provides an optimal environment for metal printing. The average inert gas consumption is less than 3 L/min, contributing to efficiency and resource conservation. Operating on a 64-bit Windows 10 system and equipped with comprehensive software including BuildStar and MakeStar®, the FS421M offers user-friendly interfaces for both advanced users and everyday operations. Supporting the STL data file format, it ensures compatibility with common 3D printing files. The power supply varies depending on region-specific standards. Operating within an ambient temperature range of 22-28°C, the FS421M accommodates diverse working environments. Materials compatible with the system include 316L, HX, HAYNES 230, IN718, IN625, AlSi10Mg, AlMgScZr, TA15, Ti6Al4V, CuSn10, with ongoing developments for additional materials in the build process. The FS421M emerges as a versatile and technologically advanced solution, embodying efficiency, precision, and flexibility in the realm of continuous metal additive manufacturing.

### **3.6 Material Properties of SS-316L**

The material properties of SS-316L, a corrosion-resistant austenitic stainless steel, are notable for their significance in various industrial applications. SS-316L, an alloy of iron, chromium, nickel, and molybdenum, exhibits a range of properties that make it highly sought after. Its exceptional corrosion resistance, even in aggressive environments, is a standout feature, rendering it suitable for applications in chemical, marine, and medical industries. With a low carbon content, SS-316L also offers improved weldability and

resistance to sensitization during prolonged exposure to elevated temperatures. The alloy showcases impressive mechanical properties, including high tensile strength, good ductility, and excellent toughness, making it ideal for structural components. Moreover, SS-316L demonstrates superior creep and stress rupture strengths at elevated temperatures. Its versatility is further accentuated by its ability to withstand a wide range of temperatures, from cryogenic conditions to moderately high heat. These material properties collectively position SS-316L as a reliable and durable material for diverse engineering and industrial applications.

### **3.6.1 Stainless Steel Alloys**

Stainless steel alloys, comprising a diverse array of materials, showcase unique properties that contribute to their extensive utilization across various industries. Recognized for their corrosion resistance, these alloys, typically consisting of iron, chromium, nickel, and other alloying elements, establish a protective oxide layer on their surfaces, safeguarding them against rust and corrosion. Exhibiting outstanding strength, durability, and longevity, stainless steel alloys are indispensable in applications where structural integrity is of utmost importance. Their exceptional heat resistance ensures the maintenance of properties across a wide temperature spectrum. Moreover, these alloys are esteemed for their hygienic attributes, finding prevalence in the food and medical industries. Versatile in various fabrication processes, they allow for intricate designs and shaping. Additionally, stainless steel alloys frequently possess favorable mechanical properties, including high tensile strength, ductility, and toughness. These collective characteristics position stainless steel alloys as versatile and reliable materials, adaptable to diverse applications in construction, manufacturing, healthcare, and beyond.

The evolution of stainless-steel alloys has been marked by advancements driven by specific material requirements. Originally, SS302, chosen for superior strength and corrosion resistance compared to vanadium steel, served as the primary stainless steel in various applications. The limitations of vanadium steel, especially in terms of corrosion resistance, led to its discontinuation in implants and the aerospace industry. Addressing corrosion concerns in chloride solutions, 18–8Mo stainless steel, incorporating a small amount of molybdenum, emerged as type 316 stainless steel. Further refinement resulted

in the development of 316L stainless steel, characterized by reduced carbon content for enhanced corrosion resistance and reduced sensitization. The addition of 11% chromium contributed to improved corrosion resistance, with passivation using 30% nitric acid enhancing this property. Austenitic stainless steels like 316 and 316L, renowned for their non-magnetic properties and superior corrosion resistance, are widely utilized in biomaterials. The molybdenum addition enhances resistance to pitting corrosion, and cold working is employed to improve hardness. The detailed composition of 316L stainless steel is provided in Table 1 (Ibrahim et al., 2017) [19].

### **3.6.2 Composition of SS-316L**

The composition of SS-316L plays a pivotal role in defining its exceptional properties and performance. The carefully balanced combination of elements, including chromium, nickel, molybdenum, and low carbon content, contributes to the alloy's remarkable corrosion resistance. Chromium forms a protective oxide layer on the surface, preventing rust and corrosion, while nickel enhances the material's ductility and toughness. The inclusion of molybdenum further fortifies resistance to pitting and crevice corrosion. Additionally, the low carbon content in SS-316L not only facilitates improved weldability but also mitigates the risk of sensitization, making it suitable for prolonged exposure to elevated temperatures. The intricate synergy of these elements ensures that SS-316L is not only durable and versatile but also well-suited for demanding applications in various industries, ranging from chemical and medical to marine and aerospace. In essence, the thoughtful composition of SS-316L underscores its significance as a high-performance material with a wide range of applications.

Both nickel (Ni) and chromium (Cr) contents significantly influence the development of the austenitic phase in 0.10% carbon stainless steel. A minimum Ni content of around 10% is essential to maintain the austenitic stage. The widely utilized 316L stainless steel in orthopedic biomaterial applications primarily incorporates three key alloying elements: chromium (Cr), nickel (Ni), and molybdenum (Mo). The addition of Cr serves to reduce environmental corrosion, while increased Ni and Mo contents enhance corrosion resistance, particularly in the chlorinated environment of bodily fluids. The "L" designation in 316L signifies a low carbon content (<0.03 wt.%), further bolstering

corrosion protection. Nickel plays a crucial role in balancing the  $\gamma$ -austenite structure, characterized by a face-centered cubic (FCC) arrangement at room temperature, contributing to the material's high toughness. The FCC structure, being more ductile than the body-centered cubic (BCC) structure, results in superior material ductility. Coarse-grained SS316L can achieve a maximum tensile elongation of up to 84%, highlighting its remarkable ductility. However, other mechanical properties, such as ultimate tensile strength and yield strength, are comparatively lower than steels with a BCC structure (Gubicza et al., 2016).

Table 2. Composition of SS-316L

Element		C	Mn	P	S	Si	Cr	Ni	Mo	Fe
SS 316L Composition, %	Min.	...	...	...	...	...	17	11	2	Balance
	Max.	0.03	2	0.05	0	1	19	14	3	Balance

### 3.6.3 Processing Parameters

The metal 3D printing process for SS-316L tensile samples involves several critical processing parameters that significantly impact the final product's quality and performance. These parameters include laser power, scanning speed, layer thickness, and build orientation. Laser power determines the intensity of the laser beam used to melt and fuse the metal powder, influencing the material's microstructure and mechanical properties. Scanning speed affects the rate at which the laser moves across the powder bed, impacting the cooling rate and, consequently, the grain structure. Layer thickness determines the thickness of each deposited layer, affecting the resolution and surface finish of the printed part. Build orientation refers to the spatial arrangement of the printed layers, influencing mechanical anisotropy and thermal properties. The importance of these parameters lies in their collective impact on the final tensile samples' integrity, strength, and dimensional accuracy. Optimizing these factors ensures the desired material properties, minimizes defects, and enhances the overall performance of SS-316L components in real-world applications.

Laser Power (W)	220
Heat Source absorption efficiency (%)	36
Laser Beam Diameter (mm)	0.12
Travel Speed (mm/s)	1050
Layer Thickness (mm)	0.03
Hatch Spacing (mm)	0.09
Recoater time (s)	10
Interlayer Rotation angle (Degree)	67
Lack of fusion temperature (K)	1300; 1600
Hot Spot temperatures (K)	2000; 3000
Interlayer Temperatures (K)	25; 600

Table 3: Processing Parameters input into the machine.

Plasticity					Temperature ©	Specific Heat
Temperature ©	Stress1 (MPa)	Plastic Strain	Stress 2 (MPa)	Plastic strain 2		
25	450	0.2	625	0.75	20	0.464
200	390	0.2	450	0.4	50	0.474
400	350	0.2	430	0.35	100	0.49
600	290	0.2	390	0.4	150	0.504
700	240	0.2	290	0.43	200	0.517
Stress Relaxation Temp ©				640	250	0.529
					300	0.54
					350	0.549
					400	0.557
					450	0.564
					500	0.57
					550	0.575
					600	0.58
					650	0.583
					700	0.586
					750	0.588
					1200	0.592

Table 4. Material Properties of SS-316L

The material properties of SS-316L, an austenitic stainless steel, exert significant influence on its performance across various applications. Notably, its exceptional corrosion resistance, particularly in chloride-rich environments, makes it indispensable for applications in marine settings, chemical processing, and medical devices. The high tensile strength of SS-316L contributes to its mechanical robustness and durability,

rendering it suitable for structural components and parts subjected to mechanical stresses. The low carbon content enhances its weldability, a crucial factor in fabrication processes, ensuring the construction of complex structures without compromising corrosion resistance. SS-316L maintains its mechanical and corrosion-resistant properties over a broad temperature range, making it apt for applications in aerospace and cryogenic engineering. Its biocompatibility qualifies it for use in biomedical applications, including implants and surgical instruments. Additionally, the material's formability allows for intricate designs, meeting diverse requirements in industries such as architecture and manufacturing. The non-magnetic properties of SS-316L further broaden its applicability, finding use in electronic components and specific medical devices. In summary, the tailored combination of corrosion resistance, mechanical strength, weldability, and other properties positions SS-316L as a versatile material meeting the specific demands of diverse applications in fields ranging from healthcare and chemical processing to aerospace and construction.

### **3.6.4 Powder Characterization**

The provided powder is a non-magnetic austenitic stainless steel characterized by its low carbon content and alloyed composition, including chromium, nickel, molybdenum, and other trace elements (refer to Table 1). Produced through the gas atomization method, this process involves the disintegration of the melt stream using nitrogen, helium, or argon under pressure. A crucible containing the charge is positioned above the atomization chamber, where the charge is heated, melted, and then sprayed through the Laval nozzle by clean gas, solidifying into fine drops. The resulting powder is collected, with the atomizer achieving up to 99.5% efficiency. Notably, the method yields a regular and spherical grain shape, contributing to its advantages.

Critical for laser application of metal powder in terms of fluidity and packing density, powder morphology is influenced by the production method. Gas atomization, plasma atomization, and plasma rotating electrode methods predominantly yield spherical particle shapes. It is generally acknowledged that plasma atomization and the plasma rotating electrode method produce more spherical particles with fewer shape irregularities, commonly known as "satellites." Research by Zhong et al. suggests that

satellites form due to variations in solidification rates between smaller molten particles adhering to partially melted particles of larger size. Understanding powder morphology becomes essential in evaluating its suitability for specific applications involving laser-based processes.

Stainless Steel 316L (SS 316L) emerges as a favored option for metal 3D printing due to several compelling factors. Renowned for its exceptional resistance to corrosion, SS 316L finds applicability across various environments, particularly those with challenging conditions, owing to its composition rich in chromium, nickel, and molybdenum. The biocompatibility of SS 316L positions it as a preferred material for medical and dental applications, making it a common choice for manufacturing implants and medical devices due to its compatibility with the human body. Withstanding high temperatures admirably, SS 316L ensures structural stability in elevated temperature settings, making it a suitable choice for applications involving heat exposure. Boasting a harmonious blend of mechanical properties, including commendable tensile strength and ductility, SS 316L proves versatile for diverse engineering and structural applications. Noteworthy for its excellent weldability, SS 316L facilitates the creation of intricate designs through processes like 3D printing. Its corrosion resistance post-welding is crucial for maintaining structural integrity. Tailored for metal 3D printing methods like Selective Laser Melting (SLM) or Direct Metal Laser Sintering (DMLS), SS 316L, in powder form, allows precise layer-by-layer printing, resulting in intricate and customized geometries. With applications spanning aerospace, automotive, and consumer goods industries, SS 316L's versatility positions it as an ideal choice for 3D printing, meeting the demands of diverse applications. In essence, the selection of SS 316L for metal 3D printing is driven by its corrosion resistance, biocompatibility, high-temperature resilience, mechanical properties, weldability, compatibility with 3D printing processes, and overall adaptability for a wide array of applications.

### **3.7. Mechanical Testing**

Tensile tests were performed for the stainless-steel dog bone samples in School of Mechanical and Manufacturing Engineering (SMME), NUST.

The mechanical testing of metal 3D printed tensile samples serves as a comprehensive examination of the material's response to applied forces, providing in-depth insights into its mechanical behavior. This rigorous evaluation involves subjecting the samples to controlled tensile forces until they reach the point of failure. Through this process, key mechanical properties are determined, including ultimate tensile strength, yield strength, elongation at break, and modulus of elasticity. Ultimate tensile strength represents the maximum stress the material can withstand, offering a measure of its overall strength. Yield strength indicates the point at which the material undergoes plastic deformation, providing insights into its elastic limit. Elongation at break measures the material's ability to deform before rupture, reflecting its ductility. The modulus of elasticity signifies the material's stiffness and its ability to return to its original shape after deformation. Analyzing these mechanical properties is crucial for assessing the material's performance in real-world applications. For instance, in aerospace, understanding the tensile characteristics ensures the printed components can endure the stress and strain experienced during flight. In medical applications, it is vital to ascertain the material's ductility and strength for the fabrication of implants or prosthetics. Moreover, the data obtained from tensile testing aids in optimizing the 3D printing process. Researchers can fine-tune printing parameters, such as layer thickness and printing speed, to enhance the material's mechanical properties. This iterative process contributes to the ongoing improvement of metal 3D printing technologies, making them more reliable and versatile for diverse industrial and scientific applications.

Tensile testing is extensively employed to evaluate the strength of materials when subjected to axial loads. This is particularly vital in scenarios where materials must endure pulling forces, such as in the construction of structural elements like buildings, bridges, or load-bearing machinery components. Compression testing is



pertinent for materials facing compressive forces, such as pillars, columns, or components supporting substantial loads. It verifies a material's capacity to resist crushing forces and maintain stability under compression. Flexural testing, also known as the bending test, is indispensable for materials used in beams, girders, or any structural component subjected to bending. It assesses the material's capability to withstand bending stresses, a critical consideration in the design of structures with specific load-bearing requirements. Shear testing is applicable to materials experiencing parallel forces, commonly found in riveted or welded joints. It determines a material's resistance to shearing forces, aiding in the design and evaluation of components subject to shear stress. Hardness testing is widely employed across various industries to evaluate material hardness, particularly crucial for applications where wear resistance is paramount. This includes selecting materials for cutting tools, gears, or any surface exposed to abrasive wear. Impact testing is essential for materials used in applications prone to sudden impacts, such as automotive parts or safety equipment. It evaluates a material's toughness and its ability to absorb energy, ensuring it can withstand sudden shocks without catastrophic failure. Fatigue testing is a critical process in industries like aerospace and automotive, where components undergo cyclic loading. This test ensures that materials can withstand repeated stress without developing cracks or failure, contributing to the longevity and reliability of components.

These tests collectively contribute to ensuring that materials meet the specific demands of their intended applications, providing valuable insights into their mechanical behavior under various conditions.

### **3.7.1 Why Hardness Test?**

The critical role of hardness testing in the domain of 3D printed metals, particularly within aerospace applications, is underlined by its multifaceted significance. Foremost, in the aerospace environment where components face elevated levels of friction and wear, hardness testing becomes pivotal in guaranteeing that 3D printed metals can withstand abrasive forces, thereby extending the operational lifespan of essential components. Additionally, as

diverse aerospace applications necessitate materials with specific hardness levels, hardness testing emerges as a decisive factor in selecting the most suitable 3D printed metal alloy that meets stringent criteria for strength, durability, and wear resistance. Furthermore, as weight reduction is paramount in aerospace engineering, hardness testing ensures that 3D printed metals maintain the delicate balance between robustness and lightweight construction, contributing to structural integrity. The test's significance extends to verifying the compatibility of 3D printed metals with harsh aerospace conditions, such as extreme temperatures and corrosive environments. In the realm of quality control, hardness testing provides quantitative data on a material's resistance to indentation and deformation, ensuring consistent and uniform quality across components. The evaluation of resistance to fatigue and cyclic loading, essential for components enduring repetitive stress, further underscores the indispensable nature of hardness testing in aerospace applications. Lastly, ensuring precision and accuracy in materials is vital in aerospace engineering, and hardness testing serves as a cornerstone, affirming that 3D printed metals meet the specified hardness values and allowing engineers to design components with unwavering confidence in their mechanical properties. In essence, hardness testing is an integral element in the intricate tapestry of aerospace engineering, ensuring materials can meet the rigorous demands of flight and uphold industry standards for safety and quality.

### **3.7.2 Tensile Test**

The significance of the tensile test in the context of 3D printed metals, particularly in aerospace applications, is profound and multifaceted. The primary importance lies in its ability to assess the strength of materials under axial loads, a crucial parameter for components subjected to pulling forces in various aerospace structures. In this realm, where structural integrity is paramount, the tensile test becomes instrumental in ensuring that 3D printed metals can withstand the dynamic forces experienced during flight, contributing to the overall reliability and safety of aerospace components. Furthermore, the tensile test is indispensable for material selection, especially in aerospace applications where specific mechanical properties are essential. By evaluating tensile strength, engineers can make informed decisions about the suitability of 3D printed metal alloys,

ensuring they meet the rigorous requirements for strength and durability imposed by the aerospace industry. Moreover, the results of tensile testing provide valuable insights into a material's behavior under stress, including its ductility and deformation characteristics. This information is vital for designing aerospace components that can withstand the complex and demanding conditions of flight. Additionally, the tensile test is crucial for quality control in aerospace manufacturing. Consistent tensile properties across 3D printed metal components ensure uniformity and reliability, crucial factors in an industry where precision is non-negotiable.

Conducting tensile testing on sandwich composite laminates is a critical aspect when considering their application in specific contexts. For this purpose, 3D printed dog-bone SS-316L specimens were prepared, following the ASTM standard, with dimensions conforming to the prescribed specifications, measuring Length – 100mm, Width-10mm, Height- 7mm, Gauge Length – 25mm and Gauge Width – 6mm. They were subjected to tensile testing in the HAIDA HD-B607-S Universal Testing Machine bearing maximum load capacity of 100 KN. A constant strain rate of 2.0 mm per minute was followed. The specimen was securely positioned between the fixtures of the UTM for conducting the test. It was subjected to a pulling force until it reached the point of failure, as depicted in Figure 12. The ultimate load applied at the moment of failure represents the ultimate tensile strength, which indicates the maximum load the specimen can withstand before experiencing failure. The step wise results of the test are discussed below in results and analysis. The ultimate strength of the specimen was determined for the maximum load carried before failure. In conclusion, the tensile test stands as a linchpin in the assessment and validation of 3D printed metals for aerospace applications. Its ability to gauge strength, inform material selection, and contribute to quality control makes it an indispensable tool in ensuring the structural robustness and reliability of components designed for the aerospace industry.

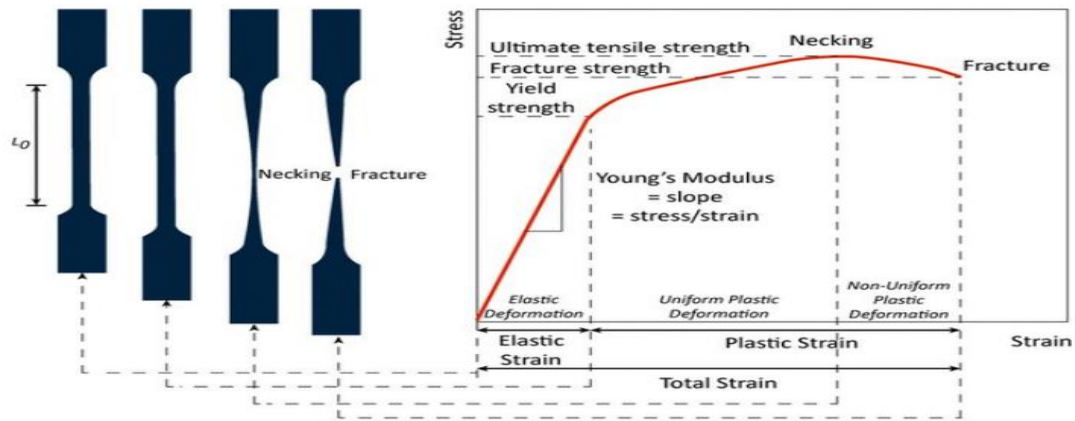


Figure 7: UTS Testing

Tensile tests are conducted to assess the mechanical properties of materials, with the Ultimate Tensile Strength (UTS) being a pivotal parameter derived from these tests. The significance of conducting tensile tests and determining UTS lies in its multifaceted applications. It serves as a crucial metric for evaluating the strength of materials under tensile forces, providing insights into their ability to withstand deformation or failure. In manufacturing, tensile testing ensures quality control by verifying that materials meet specified strength standards, maintaining consistency in production. For engineers and designers, UTS data guides material selection, aiding in the design of structures and components with a safety margin to endure expected loads. Different industries benefit from the predictive nature of UTS, allowing for the selection of materials suited to specific applications. Additionally, in failure analysis, understanding UTS helps identify the root causes of material failure and informs improvements in material selection and design for future applications. Ultimately, tensile testing and the determination of UTS play a fundamental role in ensuring the reliability, safety, and performance of materials across diverse industrial sectors.

### 3.8 Characterization

Characterization plays a crucial role in fracture mechanics analysis stainless steel (316L) alloy. The characterization process involves the detailed examination and evaluation of the material's microstructure, mechanical properties, and fracture behavior. This information is essential for understanding and predicting the

initiation and propagation of cracks in FML composites, as well as assessing their overall fracture resistance.

Characterization techniques, such as microscopy (e.g., optical microscopy, scanning electron microscopy), provide valuable insights into the internal structure of the specimen, including the arrangement grain boundaries, layer structure and the distribution of reinforcing particles. This information helps identify potential weak spots and regions of stress concentration and formation of melt pools.

### **3.8.1 Fractographic Analysis**

The Digital Microscope emerges as a crucial asset for the in-depth examination of fractographic patterns, a specialized approach focused on studying the fractured surfaces of materials to uncover the underlying mechanisms that contribute to failure. In this investigative process, the Olympus Corporation DSX10000 UZH Digital Microscope, highlighted in Figure 21 & 22, plays a pivotal role. This cutting-edge microscope is specifically chosen for its capabilities in providing detailed insights into the intricate details of the surface of the specimen near the stitching line and near the crack. The subsequent section delves into the comprehensive specifications of this microscope, elucidating its features that contribute to its efficacy in unraveling the complexities of material fracture and failure. This cutting-edge microscope stands as a testament to technological excellence, offering not only remarkable high-resolution imaging capabilities but also a carefully curated suite of features. These features are thoughtfully designed to facilitate a fluid and precise process of observing and documenting samples with the utmost detail. In the intricate world of scientific inquiry and industrial scrutiny, this microscope emerges as a powerful ally, providing a lens into the intricacies of the microscopic universe and delivering a wealth of information for researchers and industry professionals alike. This optical system boasts a diverse range of easily interchangeable lenses, providing a broad selection for various applications. With the convenience of a button, users can seamlessly switch between six observation methods, enabling swift transitions from macro to micro viewing. The tele centric optical system ensures precision in measurements, and its advanced capabilities facilitate the quick and effortless acquisition of accurate measurements.



Figure 8 & 9: Olympus Corporation DSX1000 UZH Digital Microscope

### 3.8.2 Microscopic Analysis

The scanning electron microscope (SEM) is a technological marvel, a powerhouse of precision that gracefully navigates the microscopic landscape. Armed with the ability to plunge into the infinitesimally small, the SEM is a beacon of high precision, unraveling the intricate characteristics and behaviors of a diverse array of samples at both the micro- and nanoscale. Its significance reverberates across scientific and industrial domains, becoming an indispensable tool for those seeking profound insights through in-depth imaging and analysis. The Scanning Electron Microscope in focus, specifically the ZEISS Sigma 500 VP showcased in Figure 22, exemplifies this technological prowess. Within its microscopic arena, the SEM employs various imaging modes, notably secondary electron imaging (SEI) and backscattered electron imaging (BEI). These modes act as windows into different surface properties and contrasts, unveiling a visual symphony that aids in identifying fracture modes such as fiber pull-out, matrix cracking, or interfacial debonding. This level of granularity proves invaluable in comprehending the structural integrity of Stainless Steel 316L and evaluating the grain structure and boundaries of the 3D printed metal part. The SEM, thus, emerges not just as an instrument of observation but as a key to unlocking the secrets held within the microscopic intricacies of materials, paving the way for advancements in materials science and engineering.



Figure 10: Scanning Electron Microscope (ZEISS Sigma 500 VP, NCP)

Energy-dispersive X-ray spectroscopy (EDS), also known as EDX or XEDS, stands as an analytical technique facilitating the elemental analysis and chemical characterization of materials. In this process, a sample, when excited by an energy source, such as the electron beam of an electron microscope, releases some absorbed energy by ejecting a core-shell electron. The subsequent filling of the vacancy by a higher energy outer-shell electron results in the emission of characteristic X-rays with a spectrum specific to the atom of origin. This method enables the compositional analysis of the sample volume excited by the energy source. Element identification is determined by the position of peaks in the spectrum, while signal intensity correlates with the element's concentration.

EDS elemental mapping enhances this technique by incorporating an EDS detector into an electron microscope. As the electron probe scans the sample, recorded EDS spectra are mapped to specific positions, providing compositional information at the atomic level. The quality of results hinges on a strong signal-to-noise ratio for trace element detection, enabling faster recording and artifact-free outcomes. Cleanliness is crucial, impacting the presence of spurious peaks, a consequence of materials within the electron column. In the realm of EDS materials analysis, the technique exhibits sensitivity to low concentrations, achieving minimum detection limits below 0.1% in optimal scenarios. It offers a high degree of relative precision, typically ranging from 2% to 4%. The non-destructive nature of EDS makes it applicable in most situations, requiring minimal sample preparation effort and time. With the ability to deliver comprehensive analyses of complex samples swiftly, often in under a minute, advanced and fully integrated EDS solutions are available on Thermo Scientific TEM, SEM, and Desktop systems.

### **3.9. Post Processing**

Post-processing of 3D-printed metal SS-316L is indispensable, playing a pivotal role in refining and optimizing the material for diverse applications. The significance of post-processing lies in its ability to address inherent challenges associated with 3D printing, such as surface irregularities and layer lines, through techniques like machining, polishing, or abrasive blasting, resulting in a smoother finish essential for applications where aesthetics or reduced friction are critical. Moreover, post-processing steps like heat treatment prove crucial in optimizing the material's microstructure, enhancing hardness, strength, and overall mechanical properties. This process allows for the precise adjustment of dimensional accuracy and tolerances, ensuring that the final printed parts align precisely with design specifications. Stress-relieving techniques, such as annealing, alleviate thermal stresses induced during printing, promoting dimensional stability and reducing the risk of deformation. For applications demanding enhanced corrosion resistance, post-processing steps like surface coating or specialized treatments are employed. Additionally, post-processing facilitates joining multiple 3D-printed components through methods like welding or brazing, expanding the possibilities for creating complex assemblies with improved structural integrity. Non-destructive testing methods, employed post-processing, further ensure the quality and integrity of 3D-printed metal components by detecting potential defects or inconsistencies in the printed structure. In essence, post-processing for 3D-printed metal SS-316L transforms the raw printed material into a refined, customized, and application-specific product, unlocking the full potential of additive manufacturing in various industrial domains.

#### **3.9.1. Grinding**

Grinding, recognized as a fundamental material removal process, holds substantial significance in diverse industries due to its manifold advantages. Key merits and rationales for the importance of grinding include its capacity for attaining exceptional precision and accuracy, crucial in applications where tight tolerances and superior surface finishes are imperative. The process contributes to refining the texture and appearance of materials, particularly vital in industries such as aerospace, automotive, and medical, where smooth surfaces are integral for both functional and aesthetic purposes.



Functioning as an efficient method for material removal, shaping, and achieving specific geometries, grinding is instrumental in crafting components with intricate shapes and contours. Its potential to enhance the mechanical properties of materials by optimizing surface integrity aids in defect removal, hardness improvement, and bolstering overall strength and durability. The achievement of tight tolerances is facilitated by grinding, ensuring components align precisely with specified dimensions, particularly vital in precision engineering. The process's applicability to a broad spectrum of materials, including metals, ceramics, and composites, positions it as a versatile solution for diverse material requirements. Noteworthy for its role in minimizing residual stresses and removing heat-affected zones, grinding is indispensable for components exposed to high mechanical loads, ensuring long-term reliability. The high efficiency of grinding, enabling rapid material removal, contributes significantly to increased productivity, particularly beneficial in mass production scenarios. Adaptable to a range of applications, from shaping and finishing to sharpening cutting tools, grinding's versatility solidifies its fundamental role in industries encompassing manufacturing, automotive, aerospace, and beyond. Finally, grinding assumes a crucial function in quality assurance, offering precise control over dimensions and surface finishes, thereby ensuring components consistently meet stringent quality standards. In summary, the multifaceted benefits and importance of grinding underscore its role in achieving precision, improving surface finishes, removing excess material, and contributing to the overall quality and functionality of components across diverse industries, making it an indispensable element in modern manufacturing processes.

We utilized Silicon Carbide grinding papers with a diameter of 10 inches and were employed in various grit levels, including 240, 600, 1200, 2000, 2400, and 4000. The grit level in these grinding papers is a crucial factor, as it denotes the size of the abrasive particles embedded in the paper. A higher grit number signifies finer abrasive particles, contributing to a smoother finish upon grinding. Conversely, lower grit numbers indicate coarser particles, resulting in a rougher finish but with a faster material removal rate. The grinding process was standardized, with each paper ground for 10 minutes using an automatic grinding and polishing machine operating at a head RPM of 150 CCW and Bed RPM of 250 CCW, applying a 2 DN Load. The specimen preparation methods followed ASTM E768 standards to ensure consistency and accuracy in the experimental procedure.

This meticulous approach aimed to achieve precise and reliable results in the subsequent analysis and examination.

### **3.9.2. Polishing**

Polishing of SS-316L, a pivotal step in enhancing the material's surface finish and aesthetic appeal, is achieved through the meticulous use of polishing cloth, and in this case, an automatic grinding and polishing machine was employed for optimal efficiency. The significance of polishing lies in its ability to refine the texture and appearance of stainless steel, particularly critical in industries requiring impeccable surface finishes. Utilizing polishing cloth, which can range from abrasive-embedded cloths for initial coarse polishing to softer, finer cloths for achieving mirror-like finishes, offers versatility in catering to different material requirements. The choice of an automatic grinding and polishing machine underscores the importance of precision and consistency in the polishing process. This advanced equipment streamlines the procedure, ensuring uniformity in surface finishes and minimizing the risk of human-induced variations. The types of polishing employed may include rough polishing to remove imperfections, intermediate polishing for further refinement, and final polishing to achieve the desired mirror-like surface. Each stage contributes to improving the aesthetics and corrosion resistance of SS-316L. In conclusion, polishing with the aid of polishing cloth and an automatic grinding and polishing machine plays a pivotal role in elevating the surface quality of SS-316L, meeting stringent standards for appearance and performance in diverse applications. Polishing of SS-316L, a critical phase in refining its surface quality, involved the meticulous use of polishing cloth and an automatic grinding and polishing machine. This advanced equipment ensured precision and consistency throughout the process, reducing the risk of variations. During the polishing stages, including rough polishing, intermediate polishing, and final polishing, a carefully selected sequence of polishing cloths, ranging from abrasive-embedded ones for initial coarse polishing to softer, finer cloths for mirror-like finishes, was utilized. Additionally, diamond and aluminum paste served as lubricants during the polishing process, playing a crucial role in avoiding friction and facilitating a smooth surface finish. The incorporation of diamond and aluminum paste not only enhanced the efficiency of the polishing procedure but also contributed to achieving the desired surface aesthetics and corrosion resistance of SS-

316L. This comprehensive approach to polishing, integrating advanced machinery and specialized lubricants, underscores the commitment to achieving optimal surface quality in line with the stringent standards of appearance and performance for SS-316L in diverse applications. During the final polishing stage, two types of cloths were utilized, distinguished by their micron values: 5 Microns and 3 Microns. The "3 micron" designation on the polishing cloth refers to the average size of the embedded abrasive particles. In this context, the cloth contains abrasive particles with an average size of 3 microns, serving as a critical parameter for the polishing process. The micron value offers insights into the abrasive grit size, influencing the level of surface smoothness and polishing effectiveness achieved during the polishing procedure. Smaller micron values generally indicate finer abrasives, contributing to a smoother and more refined surface finish. This meticulous polishing approach with specified micron values aimed to ensure precision and consistency in the final polishing results for subsequent analyses and examinations.

### **3.9.3 Etching**

Etching proves to be an indispensable process in both metallography and material science, serving diverse purposes in unveiling intricate microstructural details and facilitating the analysis of metallic specimens. Its significance lies in the capacity to selectively remove material from a metal surface, thereby rendering internal structures visible for microscopic examination. Several key aspects underscore the importance of etching, including its role in revealing the microstructure of metals, showcasing features like grain boundaries, phases, and inclusions. This analysis becomes paramount for comprehending the material's properties and behavior. Furthermore, etching aids in defect identification, uncovering imperfections such as cracks, porosity, or inclusions that may elude surface visibility. This proves vital for quality control, ensuring the structural integrity of metallic components. The impact of grain size on mechanical properties is substantial, and etching allows for precise visualization of grain boundaries, facilitating accurate grain size determination crucial for assessing material characteristics. Distinguishing different phases within a metal alloy, each with distinct properties, is another valuable contribution of etching, providing insights into the composition and distribution of elements within the material. In the realm of metallography, etching serves

as a fundamental precursor to microscopic examination, enhancing the contrast between diverse microstructural features and enabling detailed and accurate observations. The types of etchants employed further underscore its significance, each tailored to specific metals or alloys, and selected based on the desired details to be unveiled. In essence, etching emerges as a pivotal step in the comprehensive analysis of metal specimens, offering crucial information about their microstructure, defects, and composition. The judicious selection of appropriate etchants remains paramount, aligning with the specific metal or alloy under scrutiny and the intended details sought for revelation.

Types of Etchants and Their Purposes are as follows, Nital (Nitric Acid + Alcohol) is Widely used for general-purpose etching of steel and iron alloys. It reveals grain boundaries, carbide distribution, and other microstructural features. Picral (Picric Acid + Acetic Acid + Alcohol) is Suitable for etching aluminum and its alloys. It highlights grain boundaries, phases, and precipitation of certain constituents. Kalling's No. 2 (Copper Chloride + Hydrochloric Acid + Ethanol) is Ideal for revealing the microstructure of titanium and its alloys. It enhances the contrast between different phases and grain boundaries. Vilella's Reagent (Peroxide + Hydrochloric Acid + Water) is Used for etching stainless steels to reveal the austenitic and martensitic phases. It aids in identifying grain boundaries and precipitates. Oxalic Acid is Effective for etching aluminum and its alloys. It reveals grain boundaries and certain microstructural features. Aqua Regia (Nitric Acid + Hydrochloric Acid) is Suitable for etching refractory metals like tungsten and molybdenum. It highlights grain boundaries and other microstructural details.

In summary, etching plays a crucial role in the analysis of metal specimens, providing valuable information about their microstructure, defects, and composition. The selection of appropriate etchants depends on the specific metal or alloy under examination and the desired details need to be revealed.

In the evolution of metal and metallic compound development, chemical processing assumes a crucial role, involving wet and dry chemical etching, solid metal reactions, and diverse solutions featuring molten fluxes, molecular gases, and electrolytic procedures. These applications are tailored to address various material structures, spanning from colloidal and amorphous to crystalline and single crystal forms. Purpose-specific

solutions are formulated for tasks like general removal, polishing, and structuring. The narrative recognizes concerns about surface contamination, particularly native oxides, oils, greases, and organic residues. It emphasizes intentional oxidation for effective surface cleaning and underscores the controlled growth of oxides, nitrides, borides, and carbides, showcasing their significance as passivating elements or masks in device construction. Acknowledging the vital role of physical properties, including melting points and crystal structure, the chapter offers valuable insights into chemical processing considerations applicable to bulk materials, thin or thick films, alloys, and multilayer constructions.

Metal etching is a strategic process utilized for the selective removal of material from metal surfaces, revealing intricate microstructural features. Within this context, aqua regia, a potent mixture of nitric acid ( $\text{HNO}_3$ ), hydrochloric acid ( $\text{HCl}$ ), and distilled water in a precise 1:3 molar ratio, serves as a commonly employed etchant. Aqua regia's aggressive chemical composition enables the dissolution of metals, generating a clean and well-defined surface for subsequent analyses. The etching procedure involves immersing the metal sample in the aqua regia solution for a brief duration, typically around 5 to 10 seconds. Subsequent treatment includes spraying ethanol to eliminate residual chemicals, ensuring clarity. The final step involves meticulous drying of the sample using a blow dryer, preparing it for various analytical techniques. This careful etching process, complemented using aqua regia, is fundamental for unveiling intricate details on metal surfaces, enhancing the efficacy of subsequent examinations, and facilitating in-depth analyses. ASTM E407- metals with etchants, was utilized. For our experiment the etchant used was as follows: ZNTE-0005b ETCH NAME: Aqua regia. TYPE: Acid, preferential TEMP: RT COMPOSITION: 3 ...  $\text{HCl}$  1 ...  $\text{HNO}_3$  [20]



Figure 11: Original Samples after EDM wire cut.

EDM Wire Cut, or Electrical Discharge Machining Wire Cut, is a precision machining process used to cut intricate shapes and profiles from electrically conductive materials. In this process, a thin, electrically charged wire, typically made of brass or tungsten, is guided through the workpiece while submerged in a dielectric fluid. The wire generates a controlled electrical discharge or spark, eroding the material and creating the desired shape. EDM Wire Cut is known for its high precision and the ability to cut complex geometries with tight tolerances. In the context of preparing samples for analysis under a Scanning Electron Microscope (SEM) and a digital microscope, EDM Wire Cut serves as a method for obtaining precisely shaped and sized samples. The precision of the EDM process ensures that the samples match the desired dimensions for analysis. The electrically conductive nature of the materials used in SEM and digital microscope samples aligns well with the capabilities of EDM Wire Cut, making it a suitable method for creating detailed and accurate samples for microscopic examination. This process is particularly valuable when dealing with materials that may be challenging to cut using traditional machining methods, allowing for the production of intricate samples tailored to the requirements of SEM and digital microscope analysis.

### **3.10 Impact of Heat Treatment**

The comprehensive evaluation of material properties under the influence of heat treatments is achieved through an in-depth analysis of microstructure. This analytical approach serves as a critical framework for the examination of factors such as tensile strength, grain size, porosity, impact hardness, and ductility. Numerous research initiatives have delved into the impact of varying cooling rates on a range of material characteristics, including grain size, hardness, ultimate tensile strength, secondary phase precipitates, elongation of cast parts, secondary dendrite arm spacing, porosity, and yield strength.

Kaiser et al. observed that an escalation in cooling rate correlates with a reduction in the size and area fraction of carbides, leading to heightened hardness and improved mechanical properties like tensile and yield strength. Simultaneously, this is accompanied by a decrease in pores and ductility. The intricate relationship between cooling rate and area fraction is found to be influenced by grain size. Moreover, alloying elements, as

highlighted by Ohkubo et al., emerge as influential factors in shaping mechanical properties. Reductions in C, N, Si, Cr, and Mo, along with the addition of Ni, Cu, and Mn, result in diminished hardness and tensile strength. Key alloying elements such as Ni, Mo, and Cr play pivotal roles in determining material properties. Ni acts as an austenite stabilizer, Cr serves as a ferrite stabilizer, and Mo contributes to corrosion resistance, particularly in chlorine-based environments. Notably, the presence of the sigma ( $\sigma$ ) phase in the microstructure of SS 316L, as specified in ASTM standard F138, raises concerns due to its magnetic properties. The  $\sigma$  phase, characterized by a tetragonal crystal structure, precipitates within the temperature range of 600°C to 1000°C, leading to reduced toughness, increased hardness, and altered elongation in steels.

## Chapter 4

### Results and Analysis

#### 4.1 Tensile Strength

Tensile strength stands as a fundamental mechanical attribute utilized to quantify the utmost tensile stress a material can endure before experiencing fracture or failure. This crucial parameter is instrumental in assessing the performance and reliability of diverse materials such as metals, plastics, and composites. The process involves applying an axial load to a specimen and gauging the resulting deformation to ascertain its tensile strength, reflective of the material's capacity to withstand forces along its length. The significance of this property extends to material selection, design refinement, and quality control procedures in various industries. It ensures the secure and effective utilization of diverse structural components and products by providing a foundation for evaluating their integrity and durability.

Specimen	Stress Relieving	Heat Treatment	UTS (Mpa)	Yield Strength (MPa)	Elongation at break (%)	Elongation Rate (%)
SL	Stress Relieving Temp= 650 °C under Vacuum	Temp 900°C	575.95	327.4	57.8	47
SL		Heating Rate = 5°C/Min				
Non-SL	Furnace cooling	Heating time = 2hrs	642.45	367.52	60.7	48
Non-SL		Heating Time = 2hrs				
		Environment = Argon				
		Furnace Cooling				

Table 5: Experimental Results of Ultimate Tensile Strength, Yield Strength, % Elongation at Break (%) & Elongation Rate (%)

The specimen's characteristics, including stress relieving, heat treatment, UTS (Ultimate Tensile Strength), yield strength, elongation at break, and elongation rate, each play a crucial role in understanding and optimizing the mechanical behavior of the material.



Stress relieving is employed to alleviate internal stresses and enhance dimensional stability, particularly after forming processes. Heat treatment, integral to tailoring microstructure, is essential for optimizing hardness, strength, and ductility. The UTS provides insights into the material's capacity to withstand extreme stresses, guiding decisions for applications demanding structural integrity. Yield strength indicates the material's plastic deformation threshold, vital for scenarios where the material must endure varying loads. Elongation at break measures the material's flexibility and ductility, while elongation rate offers valuable information about its response to external forces. In concert, these characteristics illuminate the overall performance and suitability of the material for diverse applications, from corrosion-resistant structures to components subjected to dynamic loads.

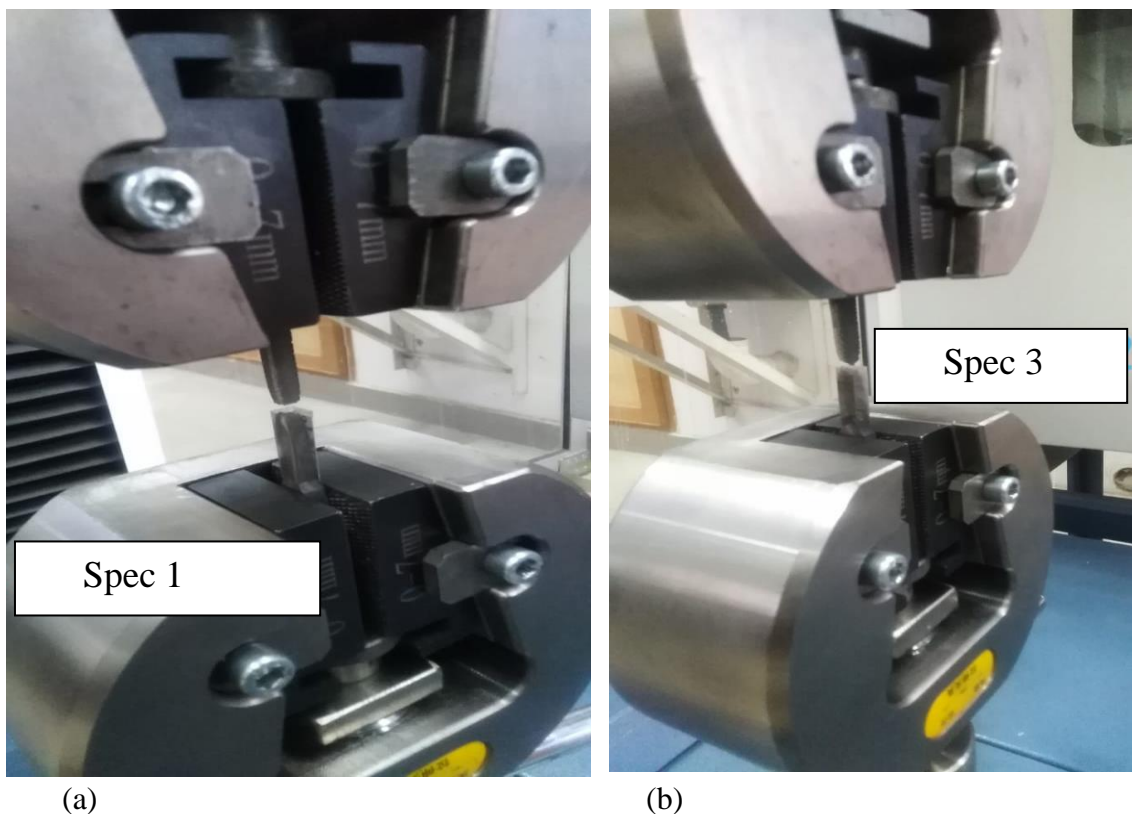


Figure 12: UTS Testing of Samples

Figure 12 (a) Spec 1 refers to sample 1 and 2, which were used for sampling after being cut using EDM- Wire Cut Machine. Similarly, figure 12 (b) spec 2 refers to sample 3 and 4 utilized for all other tests conducted. Further are the details and graphs reported in the material test.

Test Type	SPEC 1		Operator	Mohammad Umar Safir			
Mat. Name	SS		Mat. Type	SS316L/SR/HT/UTS-2 (1)			
Make Date	2022-03-25						
Temp	0	°C	Humi	0	%		
Lo	33.6	mm					
Num	Area	Fmax	Stress	Len At	Lmax	At	Fmax
	mm <sup>2</sup>	N	Max	Fmax	mm	%	Elong
			MPa	mm			Rate
							%
1	37.500	21598.4	575.95	15.669	19.72	58.7	47
Avg	37.500	21598.4	575.95	15.669	19.72	58.7	47
Median	37.500	21598.4	575.95	15.669	19.72	58.7	47

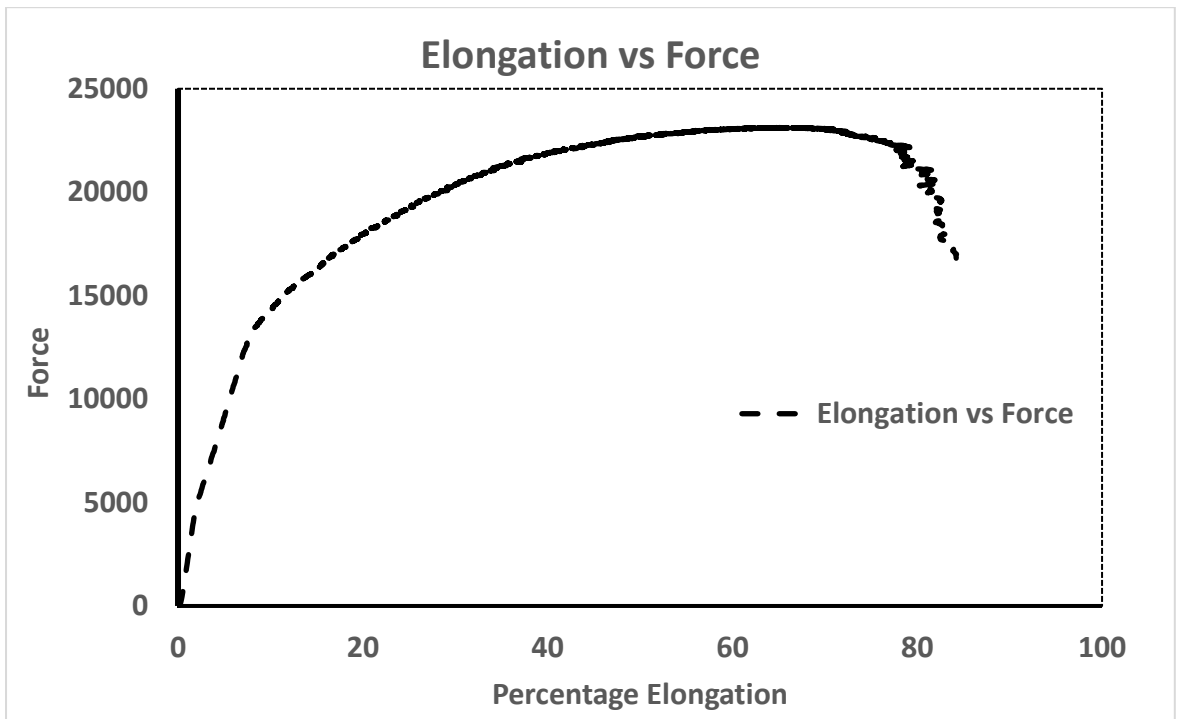


Figure 13: Force vs % Elongation

The force vs. elongation % graph obtained from the Ultimate Tensile Strength (UTS) test of SS-316L tensile samples illustrates the material's behavior under applied force

until failure. This graph provides valuable insights into the mechanical properties and performance characteristics of the material. In the initial stages of the graph, the force and elongation % are directly proportional, representing the elastic deformation region. This phase reflects the material's ability to undergo reversible deformation, reverting to its original shape once the applied force is removed. The slope of this linear region corresponds to the material's Young's Modulus, indicating its stiffness.

As the force continues to increase, the graph reaches the yield point, where plastic deformation begins. The material undergoes permanent deformation, and the force required for further elongation increases. The region beyond the yield point is characterized by strain hardening, showcasing an increase in strength despite ongoing deformation. The graph eventually peaks at the UTS, representing the maximum force the material can withstand before failure. The corresponding elongation % at this point indicates the extent of deformation endured by the material under extreme stress. Following the UTS, the graph enters the necking region, where localized deformation occurs, leading to a reduction in cross-sectional area. The force diminishes rapidly until the material reaches its breaking point, concluding the test. Analyzing the force vs. elongation % graph provides crucial information, including the yield strength, UTS, and ductility of SS-316L. It aids in understanding the material's ability to withstand applied forces, its deformation behavior, and its overall mechanical integrity. This data is essential for engineering applications where the material's strength and ductility are critical considerations.

All Heat-Treated samples in the context of this thesis, the samples have been systematically labeled in a numerical sequence ranging from 1 to 6. The purpose of this labeling is to provide a clear and organized representation of the specimens, aiding in better comprehension of their respective positions on the print bed.

1. Far from stitching line: Right View – Elevation
2. Far from stitching line: Top view – Plan View
3. Non-Stitching line sample: Near Fractured region – Right View – Elevation
4. Non-Stitching line sample: Far from Fractured region: Top View/Plan view

Non-Heat-Treated Samples:

5. Non-HT - Side View-Elevation

6. Non-HT – Top View: Plan view (Cross-section)

## 4.2. Vickers Micro-Hardness Test

The Vickers micro hardness test, conducted under specific conditions, is a pivotal examination for comprehensively evaluating material properties. In this instance, the test was performed with a force of 500 mN applied along the Z-Axis, utilizing a micro-indentation technique with a Diamond Pyramid Indenter with a 136-degree angle. The specific parameters included HV 0.05 and a dwell time of 10 seconds. These conditions ensure a meticulous assessment of the material's resistance to deformation, providing detailed insights into its mechanical behavior at the microscopic level. The results, as presented in table 3, not only quantify the material's hardness but also offer a nuanced understanding of its structural integrity. This micro hardness data becomes a crucial guide for material selection, quality control, and the optimization of mechanical properties in various engineering and industrial applications, enhancing the overall efficacy of the material under examination.

Sample	Far from SL	Center	Near SL
1. SL	322.7	289.5	269.2
3. non-SL	366.8	323.7	
5. Non – Heat Treated	232	221	

Table 6. VH Testing

The results from Vickers micro hardness testing provide valuable insights into the hardness distribution across the samples, particularly concerning their proximity to the stitching line and heat treatment status. The observed trend, where hardness increases as the sample moves away from the stitching line, suggests that the stitching process has an

impact on the microhardness of the material. This phenomenon may be attributed to the localized heat and mechanical effects during stitching, potentially causing variations in the material's hardness. Furthermore, the distinction in hardness values between the stitching line and non-stitching line samples implies that the stitching process introduces a localized hardening effect. Non-stitching line samples exhibiting higher hardness values suggest that these areas may not undergo the same level of localized hardening, resulting in a different microhardness profile.

The correlation between heat treatment and hardness values aligns with established principles, where heat treatment typically enhances the hardness of materials. The non-heat-treated samples displaying lower hardness values corroborate the expectation that heat treatment contributes to an improvement in material hardness. This reinforces the significance of heat treatment in tailoring the mechanical properties of the material. The observation of an exponential decrease in hardness values as samples move farther away from the breaking point during the UTS test is intriguing. This trend may be indicative of the material undergoing plastic deformation, which is often associated with a reduction in hardness. The gradual decrease in hardness values as the material experiences strain and deformation aligns with the mechanical behavior expected during the UTS test.

In summary, the Vickers micro hardness testing results suggest that the stitching line, heat treatment, and distance from the breaking point during the UTS test collectively influence the material's microhardness distribution. These findings contribute valuable insights into the material's response to stitching, heat treatment effects, and deformation under extreme stress, aiding in a comprehensive understanding of its mechanical properties.

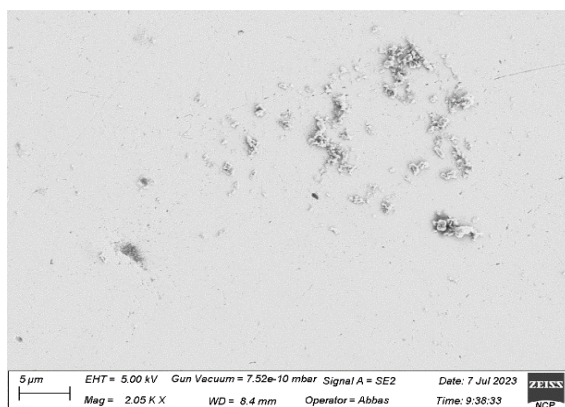
### **4.3 SEM Images of the sample:**

The in-depth scrutiny of scanning electron microscopic (SEM) images delves into the microstructural intricacies of 3D-printed SS-316L, providing a comprehensive understanding of the material's surface characteristics. Through meticulous examination, the high-resolution SEM images illustrate the topographical landscape, highlighting the granular details that contribute to the material's overall composition and mechanical behavior. Within the purview of SEM analysis, the emphasis extends to unraveling the

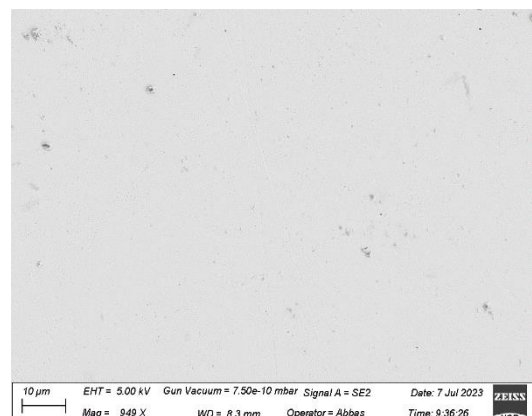
surface topography of 3D-printed SS-316L. Scanning electron micrographs not only capture the granular details but also reveal the nuanced features such as grain boundaries. The delineation of these boundaries becomes instrumental in comprehending the crystallographic arrangement and the broader structural landscape characterized by the distribution of grains. A distinctive facet of SEM examination is the discernment of surface irregularities. Pits, cracks, or other anomalous features, when identified through SEM images, provide crucial insights into potential vulnerabilities that may impact the material's performance. This microscopic exploration becomes pivotal for predictive assessments and quality assurance in the production of 3D-printed SS-316L components. Moreover, SEM analysis extends its reach to unravel morphological intricacies that contribute to the material's unique attributes. The examination of surface roughness, grain size variations, and the presence of any deposited layers adds layers of understanding to the material's composition. These morphological nuances play a significant role in shaping the mechanical behavior and structural integrity of the 3D-printed stainless steel. In essence, SEM analysis emerges not just as a visual exploration of surface features but as a sophisticated investigative tool providing profound insights into the microstructural intricacies of 3D-printed SS-316L. This comprehensive understanding is paramount for advancing knowledge in materials science, facilitating informed decision-making in industrial applications, and driving innovation in additive manufacturing processes.

Figures 14: SEM Images (a – l)

1. Away from stitching line: Right View – Elevation

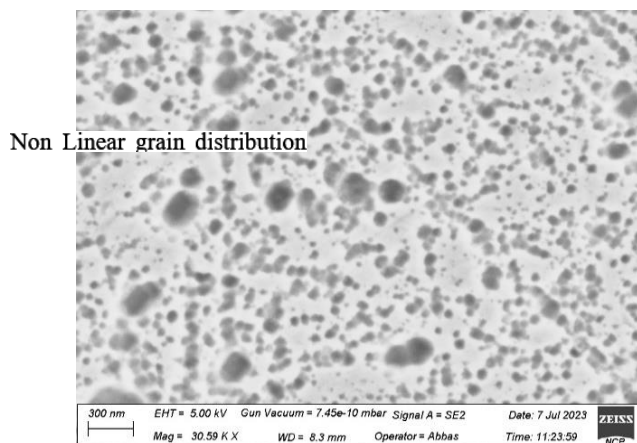


(a)

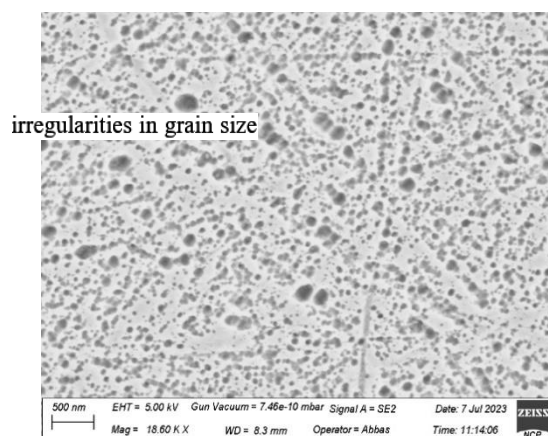


(b)

2. non-stitching line sample: Near Fractured region – Right View – Elevation

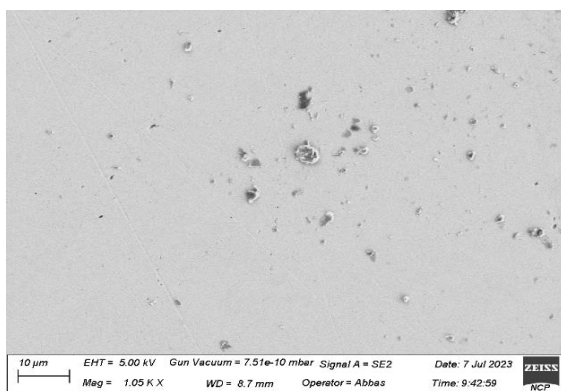


(c)

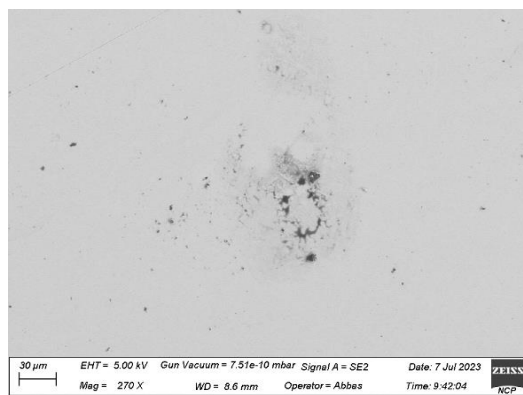


(d)

3. Stitching line samples.

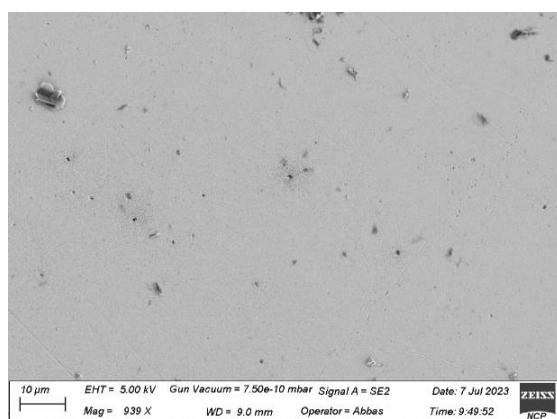


(e)

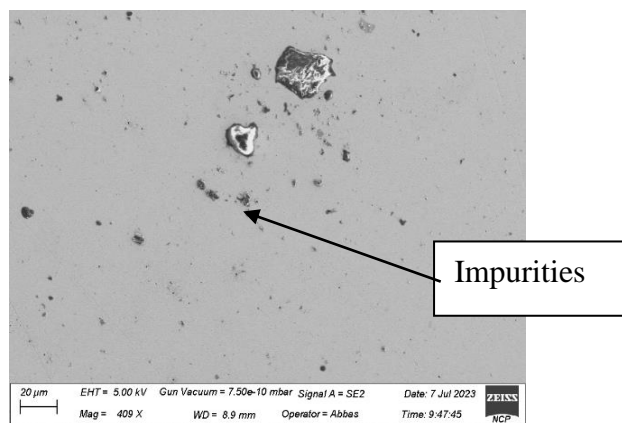


(f)

4. non-stitching line sample: Far from Fractured region: Top View

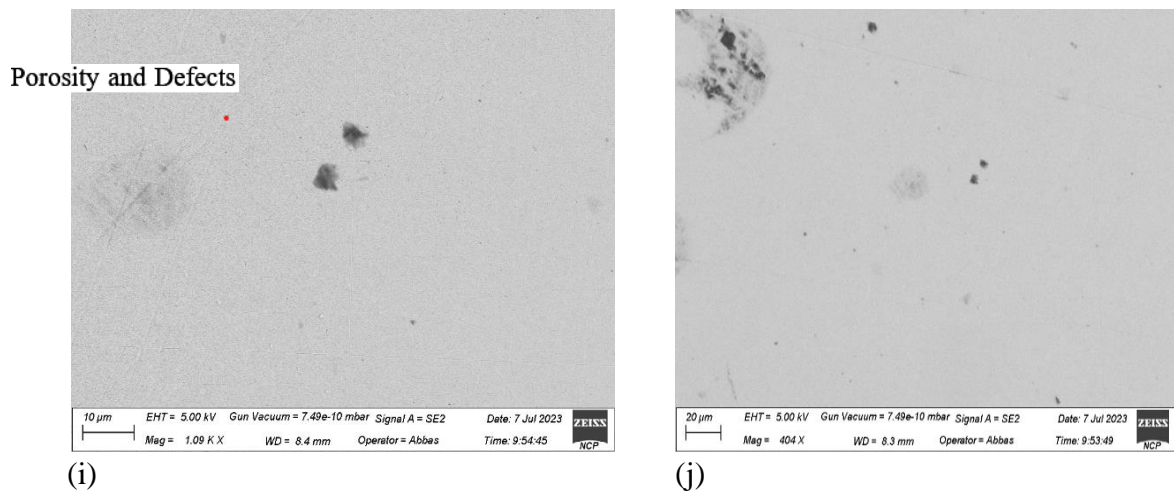


(g)



(h)

## 5. Non-HT - Side View-Elevation



## 6. Non-HT – Top View: Plan view (Cross-section)

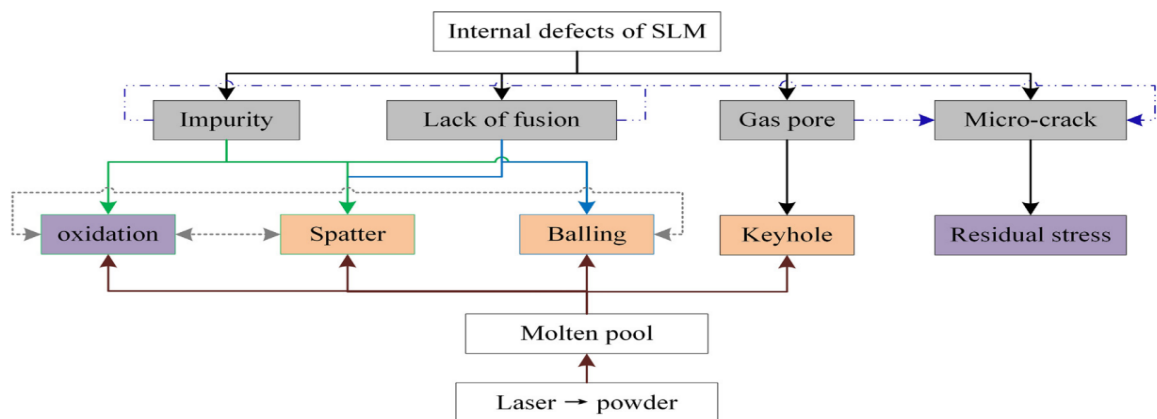
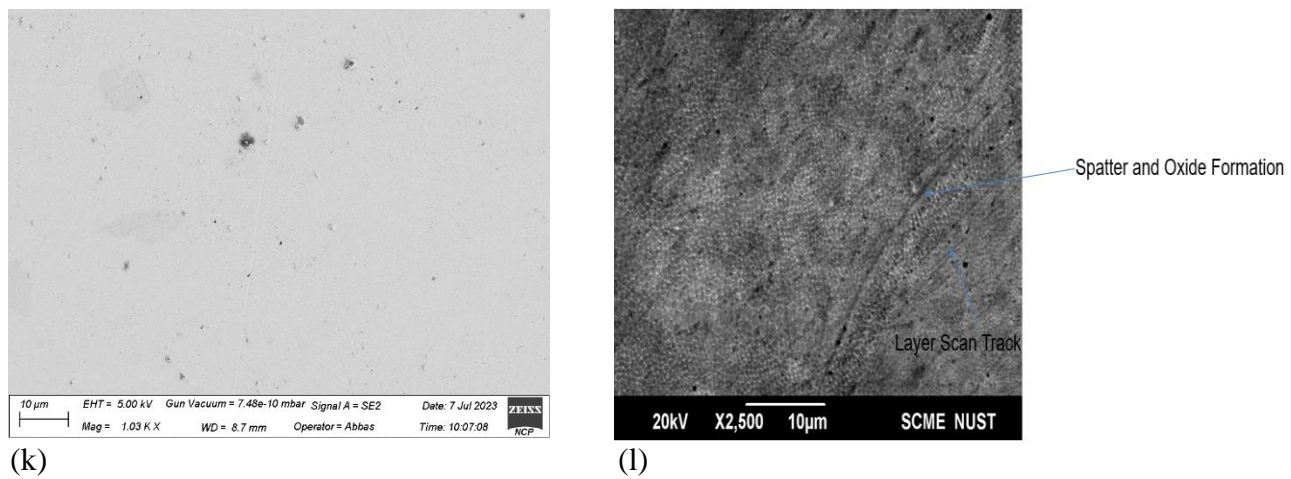


Fig.15 Defects involved in SLM Printing



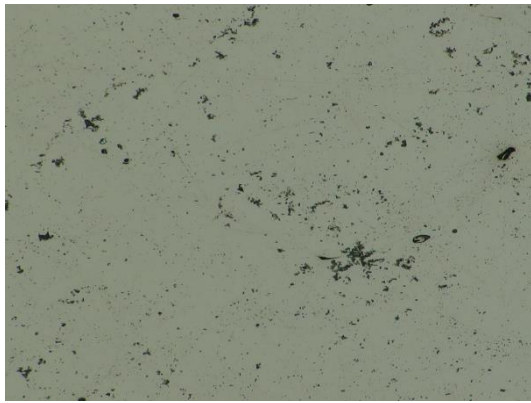
Presence of Impurities and Micro-Cracks in the context of actual Selective Laser Melting (SLM) preparation, impurities are commonly identified as oxides. These oxides often stem from the native oxide film present on the powder [21–24]. Notably, research by Liu et al. [25] has shown that large spatter particles can serve as impurities in the SLM process. Similarly, Zhou et al. [26] concluded that oxidation plays a detrimental role in balling during SLM. The presence of oxygen can influence the phase transformation temperatures, subsequently impacting the melt pool [27]. Observations by Leung et al. [28], utilizing situ X-ray imaging on invar36 alloy, highlighted the defects and melt pool dynamics. The findings underscored that oxides have the potential to act as a source for pore formation, facilitating the convection of metal solutes. These pores, in turn, migrate to the bottom of the melt pool and coalesce into larger pores. The inadequate interface combination of oxides and the melting alloy makes the generation of microcracks more prone [29]. Consequently, the investigation into defects arising from oxide impurities is intricately linked to phenomena such as balling, spatter, and the occurrence of microcracks. SLM, a powder bed additive manufacturing method, is prone to the development of internal cracks within components [30,31]. These cracks arise due to stress induced by the rapid melting of powder and are associated with factors such as excessive temperature gradients and material brittleness [32,33]. According to Zhang et al. [34], the formation of cracks is closely linked to the residual stress generated by high temperature gradients. Cai et al. [35] affirmed that harmful elements like phosphorus and silicon contribute to the creation of inter-crystalline liquid films, leading to thermal cracks. Braun et al. [36-38] concluded that oxides located at the melt pool (MP) front weaken the binding force by existing on crystal boundaries. Zhu et al. [39] demonstrated that, in a colder freezing region, spatter falling with local stress impurities facilitates crack formation. The initiation sources for crack formation, as indicated by the accumulation of residual stress, are zones with impurities, lack of fusion, and gas pores [40-41]. Consequently, preventing micro-cracks involves minimizing impurities, addressing lack of fusion, and mitigating gas pores in the SLM process.

#### **4.4 Digital Microscopic Images**

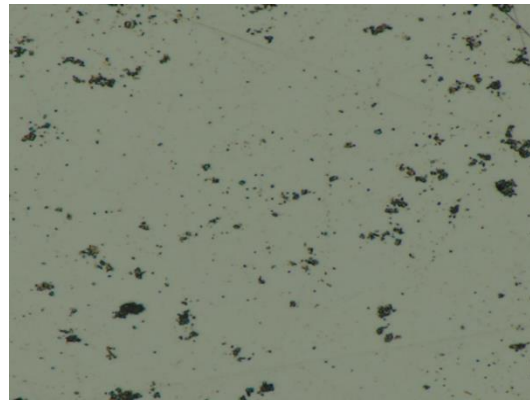
In the scrutiny of digital microscopic images explaining the microstructure of 3D-printed SS-316L, a precise analysis unveils a nuanced narrative capturing the intrinsic characteristics of the material. The microscopic examination primarily centers on recognizing the crystalline structure, evaluating the fine-grained composition, and extrapolating insights into the alloy's mechanical properties. A thoughtful examination of these images reveals a well-defined microstructure characterized by fine-grained patterns. These grains, composed predominantly of iron and alloying elements such as chromium, nickel, and molybdenum, offer pivotal indicators of the material's structural integrity. The presence of dendritic structures within the micrograph provides valuable information about the solidification process, delineating the thermal history and cooling rates inherent to the 3D printing methodology. Integral to the quality assessment and a feature that can be used to differentiate and compare two different samples is the absence of porosity or voids in one sample which is heat treated and a sample placed vertical to the recoater direction (90 Degrees), as these microscopic imperfections can undermine the material's mechanical robustness. Pore-free and uniform structures are imperative for ensuring the material's reliability and overall performance. Concurrently, any obvious defects, such as cracks or inclusions, porosity and non-continuous layer and grain size formation, warrant thorough attention, as they can significantly compromise the structural integrity of the 3D-printed SS-316L. The overarching objective of this microscopic scrutiny is to unravel the intrinsic characteristics governing the mechanical prowess of 3D-printed stainless steel. A well-tempered microstructure with refined grains is indicative of heightened mechanical properties, including enhanced hardness, strength, and ductility.

In summation, the analysis of digital microscopic images of 3D-printed SS-316L encompasses a comprehensive investigation into the material's microstructure, incorporating an evaluation of grain morphology, dendritic formations, and the absence of imperfections. This microscopic discourse serves as a foundational pillar in interpreting the material's creation and confirming its mechanical attributes, concluding in a coherent narrative for academic inquiry and technological advancement.

Figure 16: Digital Microscopic Images (a – h)

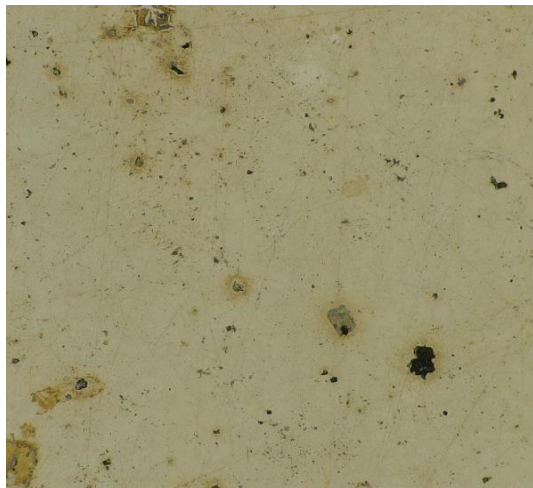


(a) Far from SL: Right View – Elevation

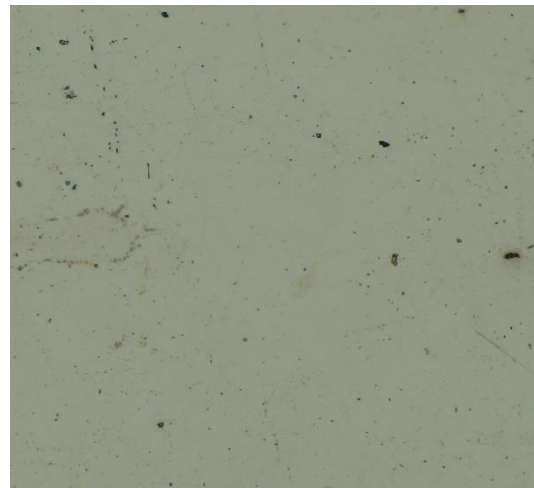


(b) Right View – Elevation

(a) & (b) Near fracture region.

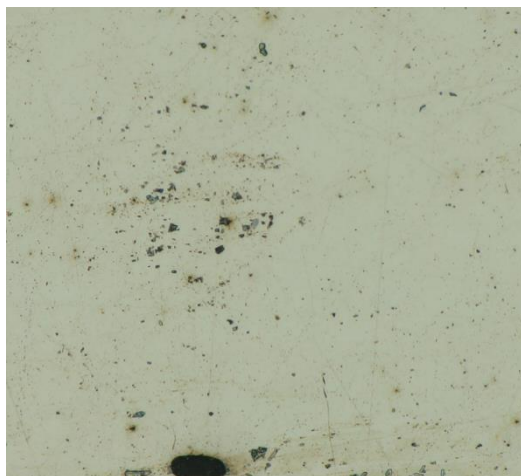


(c) SL

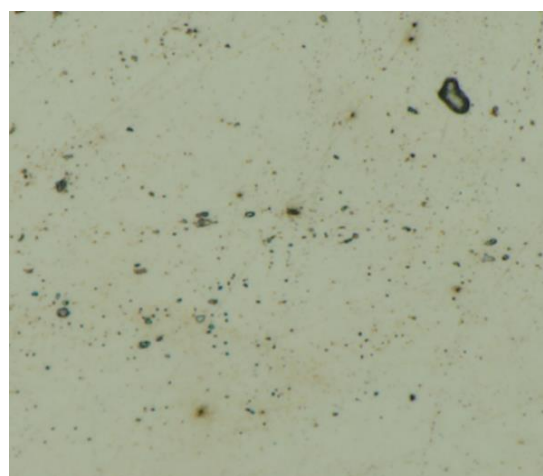


(d) 3. Non-SL: Right View – Elevation

(c) & (d) Near Fractured Region

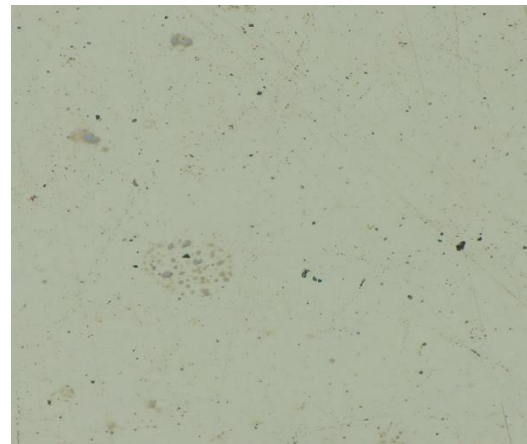
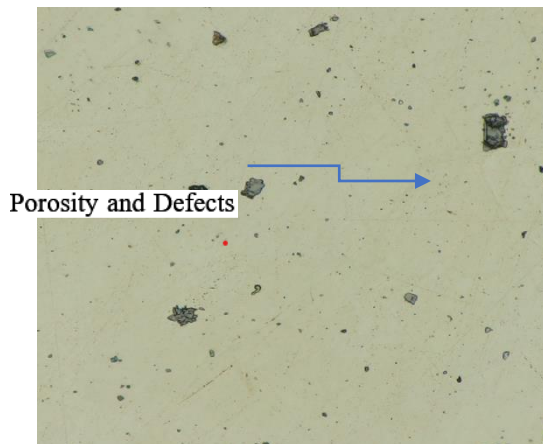


(e) Non-SL: Top View/Plan view



(f) Top View/Plan view

(e) & (f) Far from Fractured region



(g) Non-HT - Side View- Elevation

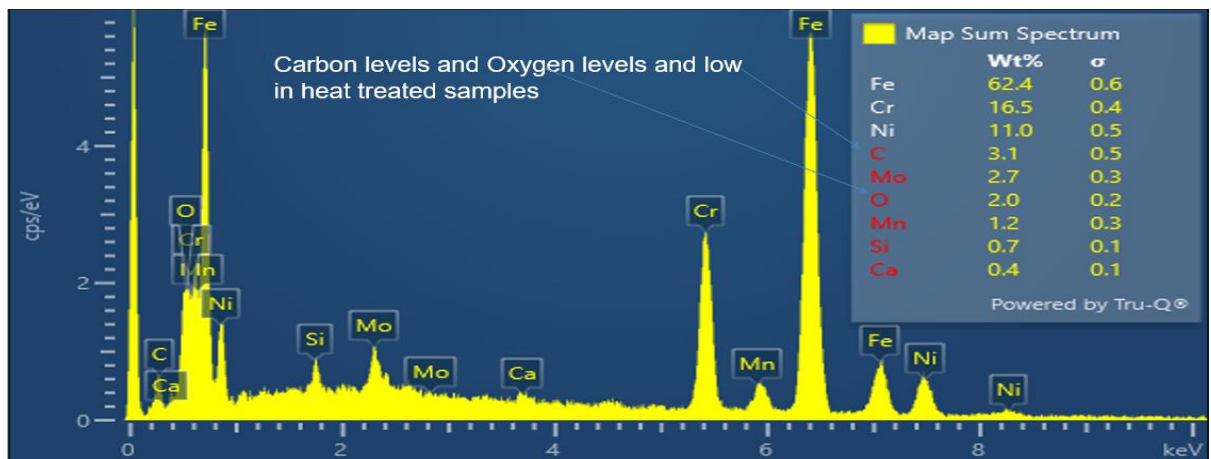
(h) Non-HT – Top View: Plan view

#### 4.5 Energy-dispersive X-ray spectroscopy (EDS) Images

The examination of Energy-Dispersive X-ray Spectroscopy (EDS) images in conjunction with scanning electron microscopy (SEM) serves as a powerful analytical tool, unraveling elemental composition and spatial distribution within 3D-printed SS-316L. The acquisition of these high-resolution EDS images enhances our understanding of the material's chemical makeup, providing crucial insights into its composition and potential variations. EDS images obtained during SEM analysis depict the elemental distribution across the sample's surface. Each pixel in the image corresponds to a specific elemental composition, enabling a detailed mapping of the distribution of elements within the microstructure of the 3D-printed stainless steel. This spatially resolved elemental analysis is invaluable for discerning variations in alloying elements, identifying potential impurities, and understanding the elemental interplay that influences the material's properties. The importance of EDS images lies in their ability to complement the structural information derived from SEM micrographs. While SEM provides topographical details, EDS adds a layer of chemical information, offering a holistic view of both the morphology and elemental composition. This integration facilitates a comprehensive characterization of the material, aiding researchers and engineers in optimizing processing parameters, ensuring quality control, and validating the material's suitability for specific applications. Furthermore, EDS images play a pivotal role in quality assurance and defect analysis. Deviations in elemental composition, such as the

presence of unexpected elements or variations in alloy content, can be indicative of manufacturing irregularities or impurities. Identifying and addressing these issues through EDS analysis is paramount for ensuring the reliability and performance of 3D-printed SS-316L components. In summary, Energy-Dispersive X-ray Spectroscopy images obtained during SEM analysis offer a multi-faceted perspective on 3D-printed SS-316L. Their role in unraveling elemental distribution and composition adds a critical dimension to the understanding of materials, contributing to advancements in materials science and informing the optimization of additive manufacturing processes.

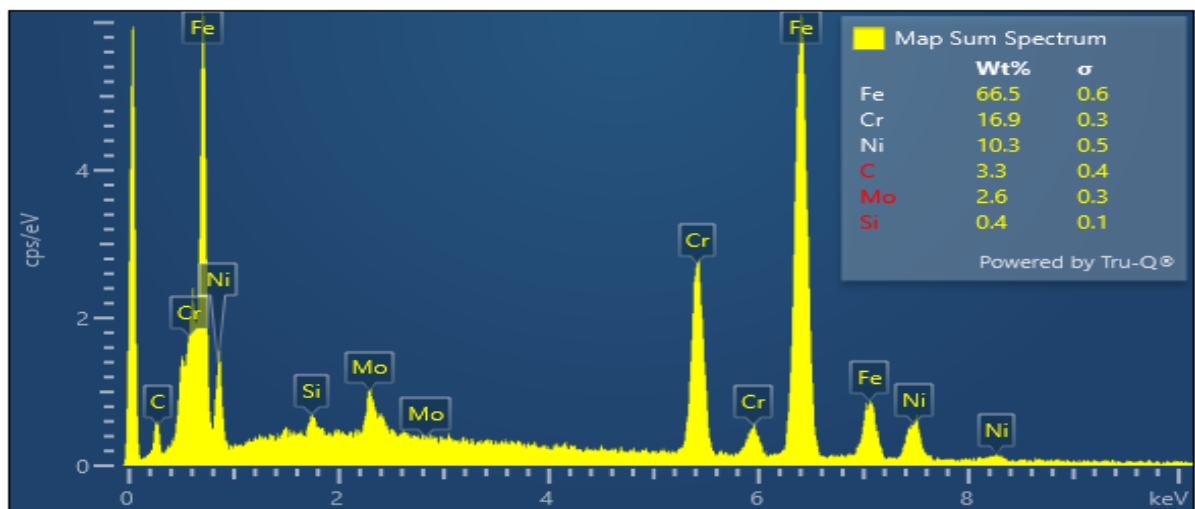
Figure 17: EDX Graphs (a – d)



Heat Treated - Far from stitching line: Right View – Elevation

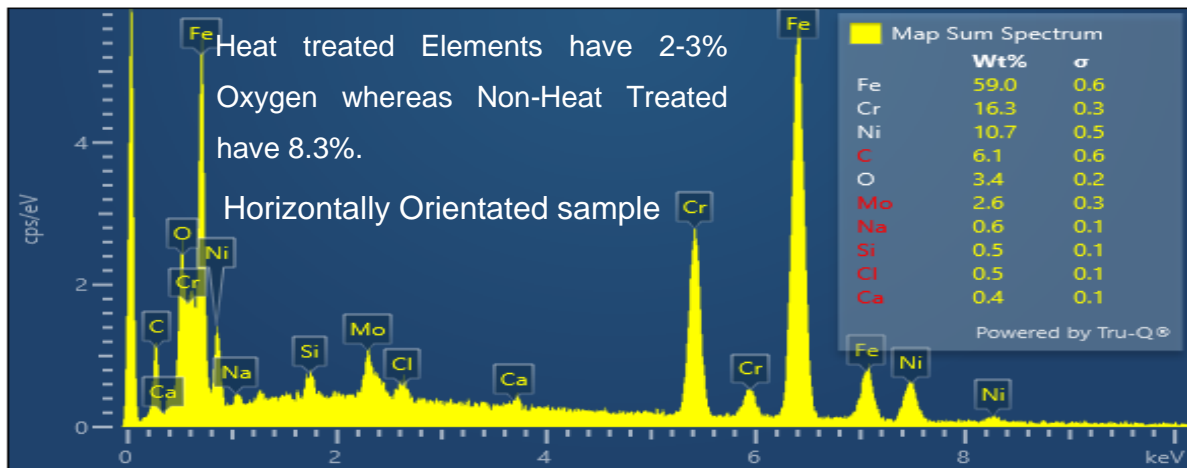
(a) EDX of specimen 1

Heat Treated - Far from stitching line: Top view – Plan View



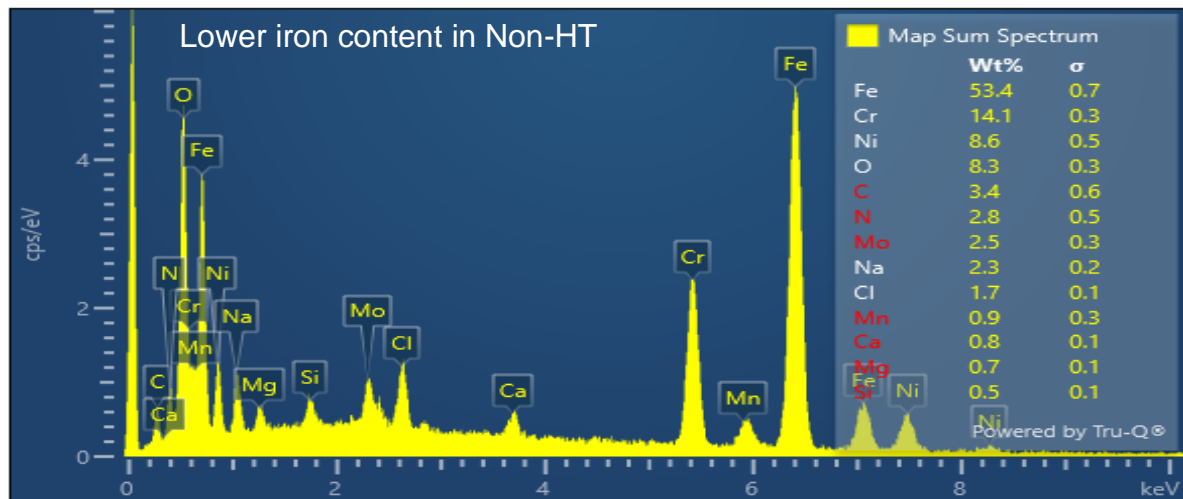
(b) EDX of specimen 2

**Heat Treated - Non-Stitching line sample: Far from Fractured region: Top/Plan view.**



(c) EDX of Specimen 4

**Non Heat Treated – Top View: Plan view (Cross-section)**



(d) EDX of specimen 5

The adjustment of oxygen levels resulting from heat treatment carries significant implications for shaping the mechanical and corrosion-resistant characteristics of metal components, notably in materials like stainless steel, exemplified by SS-316L. The heat treatment process entails subjecting the metal to controlled heating and cooling procedures, and the regulation of oxygen levels during this treatment imparts specific advantages to the material. A crucial aspect involves reducing oxygen content, often

accomplished through methods such as annealing in a controlled atmosphere or vacuum. This controlled decrease in oxygen levels serves various purposes:

Reducing oxygen content during heat treatment enhances the corrosion resistance of stainless steel, mitigating the formation of oxide layers and diminishing susceptibility to corrosion. This is particularly crucial in applications where the metal is exposed to aggressive environments, such as in marine or chemical industries. The oxygen content can impact the formation of undesirable phases in the metal's microstructure. Through controlled reduction, heat treatment stabilizes the desired microstructure, facilitating the development of phases that contribute to improved mechanical properties and overall material stability. Elevated oxygen levels during heat treatment can result in the formation of oxide scales on the metal surface, compromising aesthetics and impacting the material's mechanical integrity. The management of oxygen levels helps prevent or

minimize the formation of these scales, ensuring a smoother and more controlled surface finish. The controlled reduction of oxygen content optimizes mechanical properties such as hardness, strength, and ductility. This is achieved by minimizing the formation of oxygen-related defects within the crystal lattice, which can adversely affect the material's performance. In summary, the meticulous control of oxygen levels during heat treatment plays a pivotal role in tailoring the properties of metal components, particularly in materials like SS-316L. This control contributes to improved corrosion resistance, stabilization of microstructure, prevention of oxide scale formation, and enhancement of mechanical properties, ultimately ensuring the material meets the specific requirements of its intended applications.

The lower iron content observed in non-heat-treated elements of SS-316L introduces a noteworthy distinction in the material's mechanical properties compared to its heat-treated counterparts. In instances where the iron content remains comparatively reduced due to the absence of heat treatment, the material exhibits a relative weakness. Heat treatment plays a pivotal role in enhancing the strength and durability of stainless steel by optimizing its microstructure and elemental composition. The reduced iron content in non-heat-treated elements may result in a less robust crystal lattice and compromised mechanical integrity, impacting factors such as hardness and tensile strength. This

disparity underscores the critical role of heat treatment in fortifying the structural attributes of SS-316L, emphasizing the importance of carefully tailored processing methods for achieving optimal material performance in diverse applications. In the context of this research, the orientation of samples has emerged as a pivotal factor influencing material properties, with horizontally placed samples demonstrating superior strength and mechanical attributes compared to their vertically oriented counterparts. The horizontal arrangement, characterized by a more uniform heat distribution and gravitational influence, has led to a notable enhancement in the overall mechanical performance of the materials. These horizontally placed samples exhibit not only heightened strength but also boast a more refined grain structure and layering. The distinct advantage lies in the optimized grain orientation and layering patterns, contributing to improved structural integrity and resilience. Consequently, the findings underscore the significance of sample orientation in tailoring material properties for the specific application at hand, with horizontally placed samples emerging as the preferred configuration for enhanced mechanical prowess and structural robustness.



## Chapter 5

### Conclusion and Recommendations

#### 5.1 Conclusion:

This research about Correlation of Part Orientation during 3D Printing and mechanical properties of stainless-steel alloys is completed in a step-by-step manner from literature review to performance evaluation. In this research, an attempt has been made to study the effects of part location and orientation on printed and mechanical properties affected. The results demonstrate that mechanical properties were affected by the orientation and placement of the samples on the print bed. Exploring the concept of how well the layers are bonding and whether the stitching lines impact the overall strength of the printed metal object. With Regard to the location and orientation following conclusions were made from this research. The comparison between samples positioned along the Stitching Line and those at the center of the Print-Bed shows evident differences in mechanical and structural properties. Stitching Line samples exhibit lower Ultimate Tensile Strength (UTS), Elongation rate, and percentage of Elongation in contrast to their counterparts positioned at the center of the Print-Bed. Moreover, Vickers Hardness is notably diminished for Stitching Line samples, exhibiting an increase as one moves away from the stitching line. Further examination through SEM Images and Digital Microscopic images accentuates these distinctions, revealing irregularities in size and distribution near the stitching line that are absent in non-Stitching Line samples. Noteworthy differences in elemental composition are also evident between Heat Treated and Non-Heat-Treated elements, with the former containing 2-3% oxygen and the latter possessing 8.3% oxygen. Collectively, these findings offer a comprehensive insight into the nuanced impact of stitching and heat treatment on both the mechanical and microstructural attributes of the samples.

With regard to the samples that were heat treated and the samples that were non heat treated, the research conducted shows noticeable changes in values of the tests conducted explained in the following paragraph. The application of Heat Treatment stands as a crucial factor in elevating the strength of our materials. The heightened oxygen content

facilitates efficient absorption of high-density laser energy by the metal powder under the laser's influence, leading to a quick temperature increase. However, this increased oxygen content also introduces a challenge, making the part more susceptible to oxidation. The comparison of Vickers Hardness reveals a lower value for Non-Heat-Treated elements. Furthermore, scrutiny of SEM Images and Digital Microscopic images exposes Microstructure Non-Uniformity in the Non-Heat-Treated samples. Notably, these images vividly illustrate the presence of porosity and defects in the Non-Heat-Treated samples, providing a visual representation of the structural distinctions. This comprehensive analysis, spanning from the impact of Heat Treatment on strength to the microstructural variations depicted in images, forms a holistic understanding of the material characteristics under distinct treatment conditions. The placement of parts during metal 3D printing, also known as build orientation, is a critical aspect that can significantly impact the final quality and performance of the printed objects. Here are some points highlighting the importance and potential novelty in part placement: Minimizing Supports and Strategic part placement can help minimize the need for support structures which not only saves material but also decreases post-processing time and effort. The orientation of a part can affect how heat is distributed during the printing process, optimizing part placement can help in managing heat more efficiently, reducing the risk of thermal distortion and improving print accuracy, avoiding the formation of spatter and oxide formation.

The orientation of a part in relation to the building direction can influence its mechanical properties. Novel approaches to part placement can be designed to enhance specific mechanical characteristics, such as strength or flexibility, which can further help to mitigate residual stresses in the printed object which is crucial for preventing warping and ensuring dimensional accuracy. Efficient part placement can contribute to reducing overall printing time. Novel algorithms or methodologies for optimizing part orientation can lead to time savings in the additive manufacturing process which can lead to reduced energy consumption during the printing phase. Tailoring part placement for specific applications or requirements can be a novel approach. Parts with intricate or complex geometries may benefit from novel part placement techniques. Creative orientations can simplify printing challenging geometries, enhancing the manufacturability of complex designs. In summary, the importance and novelty in part placement during metal 3D

printing lie in the potential to optimize various aspects of the additive manufacturing process, ranging from mechanical properties and surface finish to efficiency and customization for specific applications. Creative and strategic thinking in this area can lead to advancements in the field.

## **5.2 Recommendations:**

Prospects for future research in the realm of additive manufacturing of metals are abundant, given the expanding applications in our rapidly evolving world. An intriguing avenue for exploration involves studying the impact of build orientation perpendicular to the print bed in different angles. This would take a lot of time and effort but will give the optimum angle at which the part could achieve maximum strength and have properly fused layers with microstructure showing grains and boundary lines to be perfect according to requirement, this could yield valuable insights. Another promising direction is the examination of diverse stacking combinations of support structures tailored to various orientations, shapes, and applications involved during the printing, balancing.

properties and strength while ensuring cost-effectiveness and process efficiency. Despite the time-intensive nature of preparing individual samples, the potential knowledge gained from exploring varied combinations and process parameters justifies the investment. The call for further testing, encompassing compression, fatigue, and flexural tests, underscores the need for a comprehensive understanding of mechanical properties.

Moreover, the thesis advocates for detailed simulation work and testing under diverse conditions, urging researchers to delve into alternative materials for parts and support structures. This exploration is driven by the goal of achieving heightened strength in smaller and more complex parts. The applicability of this research extends to advanced models of UAVs and Aero Components, with the aim of enhancing their capabilities, durability, and resistance to external factors. This includes the pursuit of higher altitudes under elevated temperatures and pressures, along with utilization under water is targeted as improvement in the oxidation of parts with heat treatment of multiple types and different conditions can also be studied, along with the corrosion resistant property of ss-316L is high, other materials can also be researched with higher corrosion resistance and

maintain all other important aspects relating to strength and durability according to the need of the application.

Additionally, the need for thorough examination of powder and machine process parameters emerges as crucial for the progression of additive manufacturing research. In essence, the future recommendations for research in this domain encompass and target an overall and inclusive of different research areas to approach and address the evolving demands and challenges within metal additive manufacturing.

## References

- [1] Alfaify A, Saleh M, Abdullah FM, Al-Ahmari AM. Design for additive manufacturing: a systematic review. *Sustainability* 2020;22. [https://doi.org/ 10.3390/su12197936](https://doi.org/10.3390/su12197936).
- [2] Santa-aho S, et al. Additive manufactured 316L stainless-steel samples: microstructure, residual stress and corrosion characteristics after post-processing. *Metals* 2021;11(2):15. <https://doi.org/10.3390/met11020182>.
- [3] Arbogast A, Roy S, Nycz A, Noakes MW, Masuo C, Babu SS. Investigating the linear thermal expansion of additively manufactured multi-material joining between invar and steel. *Materials* 2020;13(24):5683. <https://doi.org/10.3390/ma13245683>.
- [4] V. Chaudhary, S.A. Mantri, R.V. Ramanujan, and R. Banerjee, "Additive manufacturing of magnetic materials," *Progress in Materials Science*, vol. 114, p. 100688, 2020/10/01/ 2020, doi: <https://doi.org/10.1016/j.pmatsci.2020.100688>.
- [5] S.A. M. Tofail, E.P. Koumoulos, A. Bandyopadhyay, S. Bose, L. O'Donoghue, and C. Charitidis, "Additive manufacturing: scientific and technological challenges, market uptake and opportunities," *Materials Today*, vol. 21, no. 1, pp. 22–37, 2018/01/01/ 2018, doi: <https://doi.org/10.1016/j.mattod.2017.07.001>.
- [6] Sefene EM, Hailu YM, Tsegaw AA. Metal hybrid additive manufacturing: state-of-the-art. 2022/01/31 *Prog Addit Manuf* 2022. <https://doi.org/10.1007/s40964-022-00262-1>.
- [7] Yap CY, Chua CK, Dong ZL, et al. Review of selective laser melting: Materials and applications. *Appl Phys Rev*. 2015;2(4):41101. doi:
- [8] Eyob Messele Sefene, State-of-the-art of selective laser melting process: A comprehensive review, *Journal of Manufacturing Systems*, Volume 63, 2022, Pages 250-274, ISSN 0278-6125, <https://doi.org/10.1016/j.jmsy.2022.04.002>.

- [9] Bouzekova-Penkova, A.; Miteva, A. Some aerospace applications of 7075 (B95) aluminium alloy. *Bulgarian Academy of Sciences-Space Research and Technology Institute-Aerospace Research in Bulgaria*, **2022**, 34, p. 165-179. DOI: 10.3897/arb. v34.e15
- [10] 1. Morsiya C. A review on parameters affecting properties of biomaterial SS 316L. *Aust J Mech Eng.* 2022;20(3):803-813. doi:10.1080/14484846.2020.
- [11] book {walker1990crc, title={CRC handbook of metal etchants}.
- [12] Ridwan, Ridwan & Prabowo, Aditya & Muhayat, Nurul & Putranto, Teguh & Sohn, Jung Min. (2020). Tensile analysis and assessment of carbon and alloy steels using FE approach as an idealization of material fractures under collision and grounding. *Curved and Layered Structures*. 7. 188-198. 10.1515/cls-2020-0016.
- [13] [Support grain architecture design for additive manufacturing](#) Md Ahasan Habib and Bashir Khoda *Journal of Manufacturing Processes* • October 2017
- [14] Practical support structures for selective laser melting Author links open overlay panel [M.X.Gan](#) [C.H.Wong](#)
- [15] On utilizing topology optimization to design support structure to prevent residual stress induced build failure in laser powder bed metal additive manufacturing . Lin Chenga, Xuan Lianga, Jiaxi Baia, Qian Chena, John Lemonb, Albert To
- [16] Support Structures for Additive Manufacturing: A Review Jingchao Jiang , Xun Xu and Jonathan Stringer
- [17] Part-scale build orientation optimization for minimizing residual stress and support volume for metal additive manufacturing: Theory and experimental validation ☆,☆☆ Author links open overlay panel [LinCheng](#) [AlbertTo](#)
- [18] Novel approach to optimized support structures in laser beam melting by combining process simulation with topology optimization Cite as: *J. Laser Appl.* 31, 022302 (2019); <https://doi.org/10.2351/1.5096096> Submitted: 14 March 2019 • Accepted: 14 March 2019 • Published Online: 11 April 2019
- [19] Weber, James & Wain, Andrew & Piili, Heidi & Vuorema, Anne & Attard, Gary & Marken, Frank. (2016). Residual Porosity of 3D-LAM-Printed Stainless Steel Electrodes Allows Galvanic Exchange Platinisation. *ChemElectroChem*. 3. 10.1002/celec.201600098.

- [20] Yang, G., Xie, Y., Zhao, S., Qin, L., Wang, X., & Wu, B. (2022). Quality Control: Internal Defects Formation Mechanism of Selective Laser Melting Based on Laser-powder-melt Pool Interaction: A Review. *Chinese Journal of Mechanical Engineering: Additive Manufacturing Frontiers*, 1(3), 100037. <https://doi.org/10.1016/j.cjmeam.2022.100037>
- [21] Tang M, Pistorius CP. Oxides, porosity and fatigue performance of AlSi10Mg parts produced by selective laser melting. *International Journal of Fatigue* 2017;94:192– 201. doi:10.1016/j.ijfatigue.2016.06.002.
- [22] Luca AD, Kenel C, Griffiths S, et al. Microstructure and defects in a Ni-Cr-Al-Ti  $\gamma/\gamma'$  model superalloy processed by laser powder bed fusion. *Materials & Design* 2021;201:109531. doi:10.1016/j.matdes.2021.109531.
- [23] Pu D, Mallikarjun K, Raul BR, et al. The origin and formation of oxygen inclusions in austenitic stainless steels manufactured by laser powder bed fusion. *Additive Manufacturing* 2020;35:101334. doi:10.1016/j.addma.2020.101334.
- [24] Liu Y, Yang Y, Mai S, et al. Investigation into spatter behavior during selective laser melting of AISI316L stainless steel powder. *Materials & Design* 2015;87:797–806. doi:10.1016/j.matdes.2015.08.086.
- [25] Zhou X, Liu X, Zhang D, et al. Balling phenomena in selective laser melted Tungsten. *Journal of Materials Processing Technology* 2015;222:33–42. doi:10.1016/j.jmatprotec.2015.02.032.
- [26] Tan C, Li S, Khamis E, et al. Laser powder bed fusion of Ti-rich TiNi lattice structures: Process optimisation, geometrical integrity, and phase transformations. *International Journal of Machine Tools and Manufacture* 2019;141:19–29. doi:10.1016/j.ijmachtools.2019.04.002.
- [27] Leung CLA, Marussi S, Towrie M, et al. The effect of powder oxidation on defect formation in laser additive manufacturing. *Acta Materialia* 2018;166:294–305. doi:10.1016/j.actamat.2018.12.027.
- [28] Jue J, Gu D, Chang K, et al. Microstructure evolution and mechanical properties of Al-Al<sub>2</sub>O<sub>3</sub> composites fabricated by selective laser melting. *Powder Technology* 2016;310:80–91. doi:10.1016/j.powtec.2016.12.079.
- [29] Chauvet E, Kontis P, Gault B, et al. Hot cracking mechanism affecting a nonweldable Ni-based superalloy produced by selective electron beam melting. *Acta Materialia* 2017;142:82. doi:10.1016/j.actamat.2017.09.047.
- [30] Hyer H, Zhou L, Mehta A, et al. Composition-dependent solidification cracking of aluminum-silicon alloys during laser powder bed fusion. *Acta Materialia* 2021;208:116698. doi:10.1016/j.actamat.2021.116698.
- [31] Vilaro T, Colin C, Bartout JD. As-fabricated and heat-treated microstructures of the Ti-6Al-4V alloy processed by selective laser melting. *Metallurgical and*

- Materials Transactions A-Physical Metallurgy and Materials Science 2011;42A(10):3190–9. doi:10.1007/s11661-011-0731-y.
- [32] Mercelis P, Kruth JP. Residual stresses in selective laser sintering and selective laser melting. *Rapid Prototyping Journal* 2006;12(5):254–65. doi:10.1108/13552540610707013.
- [33] Zhang H, Liu Y, Li Z, et al. Crack analysis in Ti-6Al-4V alloy produced by selective laser melting. *Tungsten* 2021;3(3):361–7. doi:10.1007/s42864-021-00100-x.
- [34] Cai W. Research on process and property of 18Ni-300 alloy manufactured by selective laser melting, Lanzhou: Lanzhou University of Technology; 2018. (in Chinese).
- [35] Braun J, Kaserer L, Stajkovic J, et al. Molybdenum and tungsten manufactured by selective laser melting: Analysis of defect structure and solidification mechanisms. *International Journal of Refractory Metals and Hard Materials* 2019;84:104999. doi:10.1016/j.ijrmhm.2019.104999.
- [36] Wang D, Wang Z, Li K, et al. Cracking in laser additive manufactured W: Initiation mechanism and a suppression approach by alloying. *Materials & Design* 2019;162:384–93. doi:10.1016/j.matdes.2018.12.010.
- [37] Kaserer L, Braun J, Stajkovic J, et al. Microstructure and mechanical properties of molybdenum-titanium-zirconium-carbon alloy TZM processed via laser powder-bed fusion. *International Journal of Refractory Metals and Hard Materials* 2020;93:105369. doi:10.1016/j.ijrmhm.2020.105369.
- [38] Zhu M, Xuan F. Fatigue crack initiation potential from defects in terms of local stress analysis. *Chinese Journal of Mechanical Engineering* 2014;27(3):496–503. doi:10.3901/CJME.2014.03.496.
- [39] Qian CL, Elambasseril J, Shou JS, et al. The effect of manufacturing defects on the fatigue behaviour of Ti-6Al-4V specimens fabricated using selective laser melting. *Advanced Materials Research* 2014;891-892:1519–24. doi:10.4028/www.scientific.net/AMR.891-892.1519.
- [40] Tammas WS, Withers PJ, Todd I, et al. The influence of porosity on fatigue crack initiation in additively manufactured titanium components. *Scientific Reports* 2017;7:7308. doi:10.1038/s41598-017-06504-5
- [41] Simchi A, Asgharzadeh H. Densification and microstructural evaluation during laser sintering of M2 high speed steel powder. *Materials Science and Technology* 2004;20(11):1462–8. doi:10.1179/026708304X3944.
- [42] Sun, Z., Tan, X., Tor, S. B., & Chua, C. K. (2018). Simultaneously enhanced strength and ductility for 3D-printed stainless steel 316L by selective laser



melting. *NPG Asia Materials*, 10(4), 127-136. <https://doi.org/10.1038/s41427-018-0018-5>

- [43] Hajnys, J., Pagac, M., Mesicek, J., Petru, J. and Spalek, F.. "Research of 316L Metallic Powder for Use in SLM 3D Printing" *Advances in Materials Science*, vol.20, no.1, 2020, pp.5-15. <https://doi.org/10.2478/adms-2020-0001>